Volume 9 | Number 12 | 21 June 2025

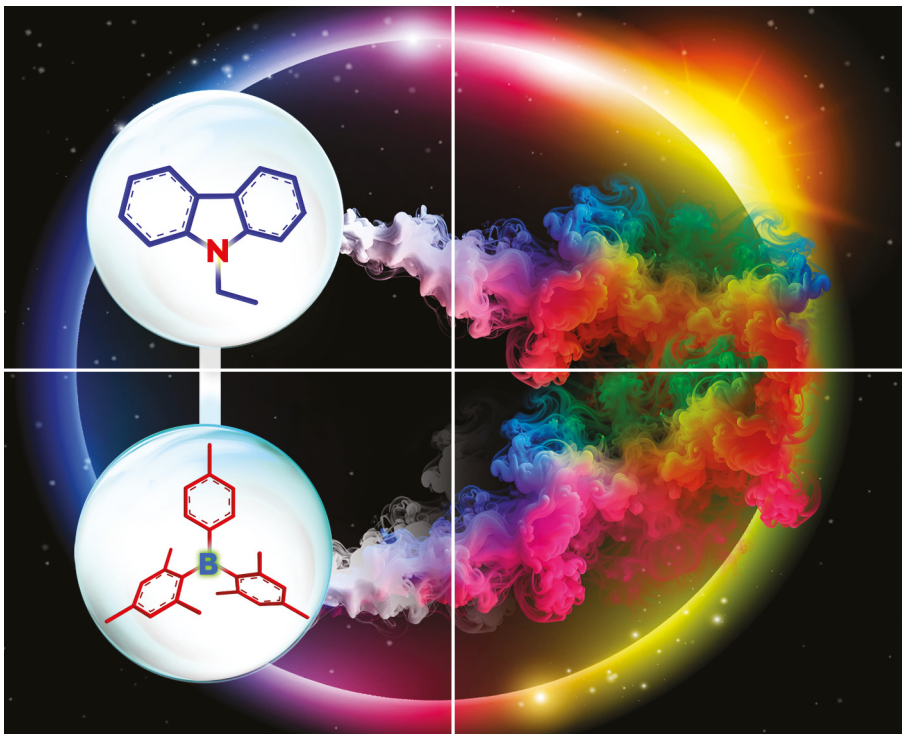

MATERIALS CHEMISTRY

FRONTIERS

CCS 中国化学会 CHINESE CHEMICAL SOCIETY
ICCAS 1956
ROYAL SOCIETY OF CHEMISTRY
rsc.li/frontiers-materials

MATERIALS CHEMISTRY
FRONTIERS

REVIEW

View Article Online
View Journal | View Issue

Cite this: *Mater. Chem. Front.*, 2025, **9**, 1794

Two decades of carbazole–triarylborane hybrids in optoelectronics

Afrin A and Chinna Ayya Swamy P *

The integration of carbazole with triarylborane has led to the development of highly efficient donor–acceptor organoboron compounds that have significantly advanced the field of optoelectronics. By combining the electron-donating properties of carbazole and the electron-accepting characteristics of organoboranes, these hybrids exhibit tunable charge-transfer characteristics, excellent photostability, and high luminous efficiency. Among these, carbazole–triarylborane systems have emerged as versatile and high-performance materials with wide-ranging applications in organic light-emitting diodes (OLEDs), thermally activated delayed fluorescence (TADF), and aggregation-induced emission (AIE). This review comprehensively covers two decades of progress in the design, synthesis, and functional exploration of these materials, discussing key breakthroughs in molecular engineering, structure–property relationships, and device integration. The review also highlights critical challenges, such as scalability, stability, and material optimization for large-scale applications. Recent advancements in data encryption technologies and computational methods are also discussed, expanding the material's scope beyond traditional optoelectronic applications. The review concludes with insights into future directions, emphasizing the growing potential of carbazole–triarylboranes hybrids in next-generation optoelectronic devices, including flexible displays, bioimaging, and sustainable energy solutions.

Received 14th March 2025,
Accepted 16th April 2025

DOI: 10.1039/d5qm00238a

rsc.li/frontiers-materials

Main group Organometallics Optoelectronic Materials and Catalysis lab, Department of Chemistry, National Institute of Technology, Calicut, 673601, India.
E-mail: swamy@nitc.ac.in

Afrin A

Afrin A obtained her Master's degree in Chemistry from Cochin University of Science and Technology in 2020. She began her research career as a Project Associate in Dr Swamy's lab in 2022 before pursuing her PhD in July 2023. Her research focuses on the modulation of solid-state emissive properties in carbazole-based donor–acceptor conjugates, aiming to develop advanced materials for optoelectronic applications.

Chinna Ayya Swamy P

Dr Chinna Ayya Swamy P obtained his MSc in General Chemistry from the University of Hyderabad in 2009 and his PhD from the Indian Institute of Science (IISc), Bangalore, in 2014, specializing in main-group organometallics. Following his PhD, he spent five years as a postdoctoral fellow abroad, in the research area supramolecular and organometallic chemistry. In 2020, he joined the Department of Chemistry at the National Institute of Technology, Calicut, as an Assistant Professor. His research focuses on the design and synthesis of novel main-group organometallic optoelectronic materials, solid-state emissive organic fluorophores for OLEDs, bioimaging, and dye-sensitized solar cells (DSSC), as well as metal-based catalysis and chemosensors for biologically relevant ions.

1. Introduction

In the rapidly evolving field of optoelectronics, the development of efficient luminescent materials capable of robust solid-state emission has been a cornerstone of innovation. These materials form the backbone of organic light-emitting diodes (OLEDs),[1–5] solid-state lasers,[6–9] bioimaging probes,[10–15] and sensors,[16–18] among other advanced applications. A critical challenge in the design of luminescent materials is addressing the aggregation-caused quenching (ACQ) phenomenon, where intermolecular interactions in the condensed phase led to non-radiative decay and diminished emission. Over two decades, researchers have tackled this issue by designing materials that exhibit aggregation-induced emission (AIE),[19] where molecular motion restriction enhances emission in the aggregated state. The demand for advanced molecular systems that offer a balance of high efficiency, strong stability, and structural tunability is driving progress in diverse applications, including full-color display technologies,[20–23] near-infrared (NIR) emitters for high-speed telecommunications,[24,25] and bioimaging solutions designed for deeper penetration and reduced light scattering.[26–29] A significant milestone in this pursuit has been the development of thermally activated delayed fluorescence (TADF) materials, which have revolutionized OLED technology.[30–34] TADF materials capitalize on their ability to convert non-radiative triplet excitons into radiative singlet states through reverse intersystem crossing (RISC), achieving internal quantum efficiencies approaching to unity. Unlike traditional fluorescent systems, TADF relies on minimizing the energy difference between singlet and triplet states, a deed accomplished through precise molecular design. This capability has set TADF materials apart, offering a new paradigm in the creation of energy-efficient and high-performing optoelectronic devices. This delicate balance necessitates precise donor–acceptor (D–A) designs, making the selection of donor and acceptor units a pivotal aspect of material design. Among the vast array of donor units explored, carbazole stands out as a versatile building block, offering an ideal platform for creating materials with exceptional optoelectronic properties.

Carbazole, a planar tricyclic aromatic heterocycle, possesses a combination of structural rigidity, strong electron-donating ability, and extended π-conjugation. These attributes, along with its inherent photostability and high thermal stability, have cemented carbazole as one of the most widely used donor moieties in organic materials.[35–42] Its electron-rich nature, derived from the nitrogen atom in the heterocyclic core, facilitates efficient charge transfer when coupled with an appropriate acceptor. This makes carbazole-based D–A systems particularly effective for luminescent applications, enabling tunable optical properties through precise molecular engineering. The rigid framework of carbazole not only ensures high photophysical stability but also aids in maintaining a planar conformation, which is essential for effective π-conjugation in solid-state emitters. Furthermore, carbazole derivatives have found significant applications in AIE materials, where their ability to restrict intramolecular motions in the solid state leads to enhanced luminescence.[42–45] Despite its many advantages, carbazole alone is not immune to the challenges of ACQ, particularly in the absence of suitable functionalization. This limitation has spurred interest in modifying carbazole with acceptor units that can enhance its luminescence properties and introduce desirable functionalities. Among the various acceptor moieties explored, organoboron compounds have emerged as highly promising candidates. Boron, as an electron-deficient element with a vacant p-orbital, brings unique electronic properties, making it a versatile acceptor in D–A systems. Its strong Lewis acidity and ability to form π-conjugated systems with electron-rich donors like carbazole enable efficient intramolecular charge transfer (ICT), which is a critical mechanism for achieving high quantum yields and tunable emission in solid-state materials.[46–50]

For several decades, organoboron compounds have garnered significant attention as electron-accepting components in donor–acceptor (D–A) systems.[51–55] The unique properties of boron, including its strong Lewis acidity and ability to participate in π-conjugation, facilitate efficient ICT, a key mechanism for attaining high quantum yields and tunable emission.[56–60] Triarylborane compounds, in particular, are noted for their strong electron-accepting capabilities and the steric protection provided by bulky aryl groups, which suppress ACQ and enhance solid-state emission. Similarly, dimesitylboron derivatives, with their steric hindrance and structural rigidity, are highly effective in promoting AIE and thermally stable photophysical behavior. These boron-based acceptors have also demonstrated remarkable potential in OLEDs,[61–63] room-temperature phosphorescence (RTP),[64–68] and advanced sensing applications.[69–73] The synergy between carbazole and boron has not only led to the development of materials with exceptional solid-state emissive properties, but also expanded their utility in cutting-edge areas such as TADF and RTP materials. These systems represent a sophisticated synergy of molecular design, combining the electron-donating ability of carbazole with the electron-accepting strength of triarylboranes. This unique interplay allows for precise tuning of photophysical and electronic properties, creating a versatile platform for pioneering material innovation. However, the development of carbazole–triarylboranes systems is not without its challenges. The inherent air and moisture sensitivity of certain boron derivatives demands meticulous synthetic strategies and rigorous handling conditions. Additionally, striking an optimal balance between stability and high performance remains a persistent hurdle. Overcoming these obstacles will require groundbreaking approaches in molecular design and advanced material engineering, paving the way for more robust and efficient applications in optoelectronics and beyond.

Our research group has been at the forefront of exploring carbazole-based materials for innovative optoelectronic and sensing applications. By examining the complementary properties of different molecular frameworks, we have uncovered new possibilities for material design and functionality. In one line of research, carbazole–cyanostilbene systems were developed to exploit the strong electron-accepting nature of cyanostilbene,

resulting in materials that exhibit remarkable AIE, mechanofluorochromic (MFC) behavior, and efficient ICT.[74–76] These studies revealed how subtle modifications in donor–acceptor interactions could fine-tune optical properties, paving the way for versatile solid-state emitters. Simultaneously, we focused our attention to triarylboranes and its conjugation with triphenylamine, focusing on their role in designing highly sensitive and selective sensors for small molecules and ions.[77–79] The inherent electron-accepting nature of triarylborane, combined with its structural flexibility, proved invaluable in achieving precise molecular recognition and signal transduction. Although these investigations began as distinct projects, they ultimately converged, demonstrating the synergistic potential of carbazole and triarylborane in molecular design. Carbazole was found to be a strong donor unit for photophysical applications, while triarylborane emerged as a versatile electron acceptor with broad functionality. This convergence has since driven our focus toward integrating these components into advanced donor–acceptor (D–A) systems, with an emphasis on creating solid-state emissive materials. Such efforts continue to bridge the gap between fundamental research and practical applications, unlocking new possibilities in optoelectronics and sensing technologies.

Our recent focus has shifted toward designing advanced carbazole-based donor–acceptor (D–A) systems featuring triarylborane acceptors. This progression reflects our commitment to develop materials with enhanced solid-state emission properties by harnessing the complementary strengths of carbazole and triarylborane. Together, these components enable the creation of materials with high photoluminescence quantum yields, stable and tunable emission profiles, and broad applicability in Frontier areas such as TADF and RTP. This review represents a pioneering effort to synthesize and analyze the collective advancements in carbazole–triarylboranes systems. Although individual studies have explored carbazole as a donor and triarylborane-based compounds as acceptors, a comprehensive perspective on their combined potential has been lacking. By bridging this gap, we aim to highlight the synergy between these molecular units and establish carbazole–triarylboranes systems as a unique platform for next-generation optoelectronic materials. We present a chronological overview of the field, beginning with foundational developments in 2006 and progressing to the latest breakthroughs. This review examines the photophysical properties, emerging applications, and the intricate structure–property relationships that define the performance of these materials. By mapping the evolution of carbazole–triarylboranes systems, we identify key milestones and emerging trends that offer valuable guidance for future research. Ultimately, this review aims to provide a comprehensive resource for scientists and engineers, illuminating the design strategies and opportunities that lie ahead. By consolidating the progress made so far, we hope to inspire new directions in the development of carbazole-based materials, unlocking their full potential for transformative advancements in optoelectronics.

2. Carbazole–triarylboranes systems: overview of key units

Combining carbazole-based donors with triarylborane acceptors has paved the way for the creation of innovative materials tailored for organic optoelectronic applications. As a versatile donor, carbazole plays a pivotal role in forming the backbone of donor–acceptor systems, while boron-based acceptors introduce unique electronic characteristics that enhance material performance. Organoboron compounds, such as triarylborane, are particularly effective as electron acceptors, offering exceptional stability and electronic versatility. These systems have proven highly impactful in applications like OLEDs, TADF, and AIE, where precise molecular tuning is key to achieve optimal functionality. This section delves into the core building blocks of carbazole–triarylboranes systems, focusing on their structural and functional contributions. By exploring the synergistic interaction between carbazole and triarylborane-based units, we aim to uncover insights into their potential as high-performance materials. Such understanding is essential for advancing the design of solid-state emitters and revealing their capabilities for future technologies.

2.1. Carbazole as an electron donor

Carbazole, a fused heterocyclic compound with a nitrogen atom in its structure, is renowned for its versatile electronic properties. The nitrogen atom contributes a lone pair of electrons, imparting strong electron-donating capabilities that make carbazole derivatives valuable in donor–acceptor (D–A) systems. These derivatives promote efficient ICT, a phenomenon crucial for tailoring the optical and electronic properties of materials, such as absorption, emission, and quantum yield.[80–82] One of the most notable features of carbazole is its ability to stabilize charge carriers, enhancing the stability and efficiency of optoelectronic materials. Structural modifications, such as adding substituents to the carbazole ring, allow fine-tuning of its electronic behavior. These modifications are especially important for applications in solution-processed devices. In addition to their tunable electronic properties, carbazole-based compounds often exhibit AIE.[83–85] Their robust thermal stability and efficient charge transport also make them essential in OLEDs, where they commonly serve as hole-transporting or emissive layers.[86,87] The design flexibility of carbazole derivatives, achieved through strategic substitutions or linkages with electron-accepting groups, enables the creation of highly efficient materials tailored for specific applications. From enhancing the brightness and color purity of OLEDs to improve the performance of sensors and solar cells, carbazole continues to play a pivotal role in advancing optoelectronic technology.[88–90]

2.2. Triarylborane as electron acceptor unit

Triarylborane compounds are recognized as accomplished materials in the field of optoelectronics due to their exceptional electron-accepting properties and structural adaptability. These compounds feature a boron atom bonded to aromatic groups, typically phenyl or mesityl (2,4,6-trimethylphenyl) groups,

which can be functionalized to tune their electronic and photophysical properties. The electron-deficient boron centre readily interacts with electron-rich donor units like carbazole, facilitating efficient ICT. The unique design of triarylboranes allows for strong fluorescence, which is further amplified by conjugation between the donor and acceptor units. The steric bulk of the aromatic groups surrounding the boron centre provides structural stabilization and reduces ACQ, enabling high emission efficiency. These systems can be further fine-tuned by introducing functional substituents on the aromatic or mesityl groups, allowing precise control over their optical properties, charge transport efficiency, and stability. The fusion of carbazole with triarylborane-based acceptors continues to drive advancements in the development of materials for optoelectronic technologies, including high-efficiency OLEDs,[51–54] photovoltaics,[91,92] and fluorescent sensors.[93–98]

3. Carbazole–triarylboranes hybrids: two decades of advancements

This section examines the evolution of carbazole–triarylboranes hybrid materials over the two decades from 2005 to 2025, drawing their journey from conceptual frameworks to impactful innovations. By focusing on breakthroughs in molecular design, structure–property optimization, and real-world applications, this review highlights the role of carbazole as a versatile electron donor and triarylborane as an efficient electron acceptor. The integration of these components has enabled significant advancements in optoelectronic materials, fostering the development of high-performance devices. This timeline captures the key milestones, challenges, and achievements that have shaped this dynamic field.

3.1. Early developments and initial discoveries

The early developments of carbazole–triarylborane hybrids encompassed both small molecule and polymer-based systems, which significantly contributed to the evolution of optoelectronic materials. Initial studies explored the synthesis of these materials, their charge-transfer properties, and their potential for efficient light emission, paving the way for advancements in OLEDs and other applications. In 2006, Lambert *et al.* reported the synthesis of amino-substituted triarylboranes (TABs), including **DP-ArB-1** and **CZ-ArB-1-2**, using copper(I)-catalyzed cross-coupling reactions (Fig. 1).[99] A key finding of this study was the ability of **CZ-ArB-2** to undergo potentiodynamic electropolymerization, forming an electroactive polymer film on the electrode surface. This polymer demonstrated electrochemical switching between neutral, oxidized, and reduced states, with fully reversible p-doping while limited stability during n-doping. Unlike **CZ-ArB-2**, the linear TABs **DP-ArB-1** and **CZ-ArB-1** primarily formed dimers upon electrochemical oxidation. This behavior suggests that in the polymerized form (poly-**CZ-ArB-2**), the TAB units are connected through carbazole-dimer linkages rather than forming extended carbazole oligomeric chains. This conclusion was supported by cyclic voltammetry (CV) data, which showed two distinct oxidation signals for poly-**CZ-ArB-2**, reflecting its unique electrochemical behavior

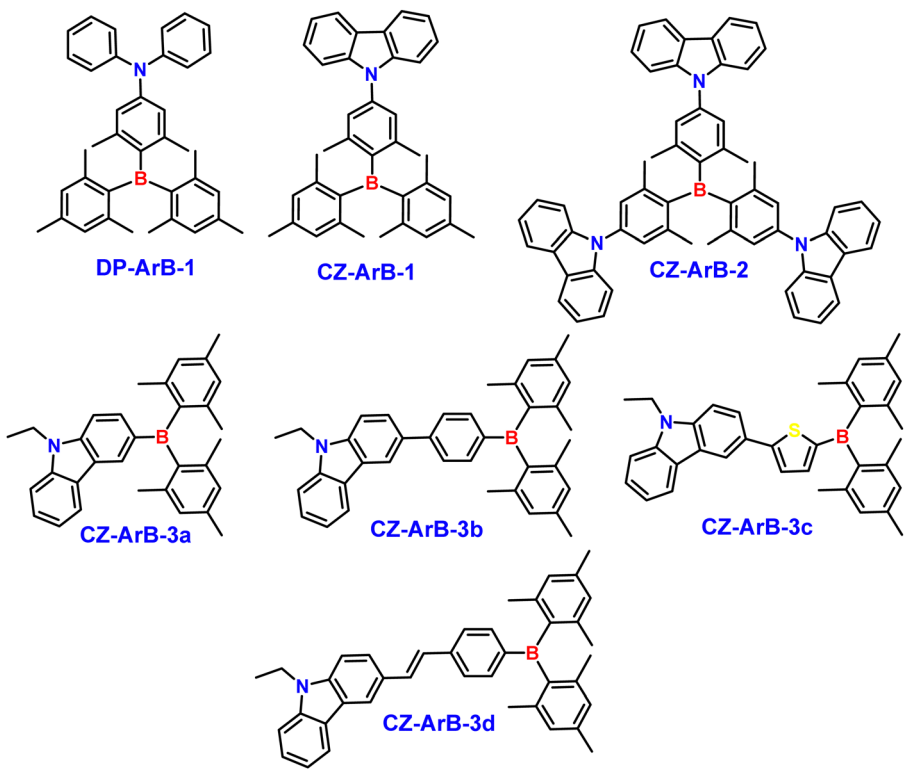

Fig. 1 Structure of compounds **CZ-ArB-1–3d**.

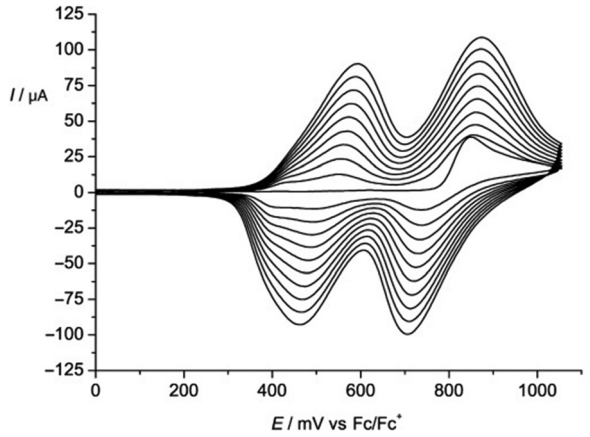

Fig. 2 Multisweep cyclic voltammetry (CV) of **CZ-ArB-2** (0.41 mM) in 0.2 M CH_2Cl_2/TBAP at a scan rate of 100 mV s^{-1} over 10 cycles. Reproduced with permission from ref. 99. Copyright 2006 Wiley.

(Fig. 2). Structurally, weak BN π–π interactions in the compounds indicate a benzoid ground-state structure with an inverted dipole moment, which becomes more pronounced during the S_0 to S_1 transition due to charge transfer (CT) from nitrogen to boron, increasing solvent reorganization energy and leading to negative solvatochromism. Interestingly, **CZ-ArB-2** deviates from the typical *D*3 symmetry of triphenylborane and related TABs, exhibiting symmetry breaking in solution. This is attributed to the rotation of its two carbazole moieties. Fluorescence anisotropy measurements revealed energy transfer between subchromophores, further emphasizing the impact of symmetry breaking on the compound's spectral properties. These unique characteristics could significantly enhance the performance of **CZ-ArB-2** and its derivatives in solid-state applications, such as OLEDs. The solvation dynamics of this highly symmetric tri-carbazole-substituted triarylborane (**CZ-ArB-2**) and less symmetric mono-carbazole-substituted triarylborane (**CZ-ArB-1**) were further investigated by Megerle and coworkers in 2008.[100] The study revealed that **CZ-ArB-2**, with its symmetric structure, exhibited faster solvation as compared with **CZ-ArB-1**, particularly in solvents with slower relaxation times. This difference was attributed to the ICT occurring within **CZ-ArB-2**, where the electronic excitation can hop between the carbazole units, enabling a quicker adaptation of the dipole moment to the solvation environment. This mechanism accelerates the solvation process by providing an additional pathway for the solute to reach its minimum-energy configuration. In contrast, **CZ-ArB-1**, lacking this symmetry and charge redistribution pathway, demonstrated slower solvation. The study highlighted how molecular symmetry and ICT influence solvation dynamics, especially in solvents with varying relaxation times.

In 2008, Jeng *et al.* reported the synthesis of four carbazole derivatives (**CZ-ArB-3a–d**) incorporating dimesitylborane and various π-conjugated bridges (Fig. 1).[101] These derivatives were designed to explore the effects of conjugation and electron-rich substituents on their photophysical properties and performance in optoelectronic devices. Among the series, **CZ-ArB-3d**, containing a styryl bridge, exhibited the longest absorption wavelength at 395 nm due to its extended π-conjugation. Similarly, **CZ-ArB-3c**, featuring a thiophene-based bridge, displayed an absorption spectrum comparable to **CZ-ArB-3d**, with a slight red-shift attributed to the presence of thiophene unit. Notably, the thiophene bridge in **CZ-ArB-3c** contributed to a narrower energy bandgap of 2.73 eV compared to the 3.01 eV bandgap in the phenyl-based **CZ-ArB-3b**, highlighting the electron-donating nature of the sulfur atom and the greater electron density of the thiophene ring relative to benzene. The introduction of conjugated bridges in the series led to a pronounced red-shift in their absorption spectra, with emission peaks ranging from deep-blue to greenish-blue (**CZ-ArB-3a** (403 nm), **CZ-ArB-3b** (443 nm), and **CZ-ArB-3d** (503 nm)). The photoluminescence spectrum of **CZ-ArB-3c** was further red-shifted to 470 nm, a consequence of the lower aromaticity and higher electron density of the thienyl group compared to the benzene ring. The OLED devices incorporating **CZ-ArB-3b** and **CZ-ArB-3c** demonstrated deep-blue and blue emissions, CIE coordinates of (0.15, 0.09) and (0.13, 0.21), respectively. These devices exhibited exceptional performance, achieving maximum external quantum efficiencies (EQEs) of 4.3% and 6.9%, with operational EQEs of 4.1% and 5.6% at a current density of 20 mA cm^{-2}. The impressive efficiency of these devices is attributed to the efficient charge confinement and optimal alignment of the HOMO and LUMO energy levels. Additionally, the solid-state fluorescence efficiencies (Φ_f) of 54% for **CZ-ArB-3b** and 51% for **CZ-ArB-3c** significantly contributed to their high EQEs. The same year, Lambert *et al.* synthesized two novel polycarbazoles, **CZ-ArB-4** and **CZ-ArB-5**, which featured a triarylborane group attached to the nitrogen atom of the carbazole unit (Fig. 3).[102] These compounds were synthesized using the Yamamoto coupling reaction, with a reference polymer (**R1**) incorporating a triarylmethyl group for comparison. The study investigated how the position of the triarylborane group within the polymer backbone influenced the materials optical and electrochemical properties. For the 2,7-linked polymer (**CZ-ArB-4**), the presence of the triarylborane group had slight effect on the absorption and emission properties. This is likely due to the effective conjugation along the polymer backbone, which maintained the electronic structure of the material. On the other hand, the 3,6-linked polymer (**CZ-ArB-5**) displayed significant changes in its optical behavior. The triarylborane group in **CZ-ArB-5** disrupted the conjugation, introducing a low-energy CT absorption band and resulting in a red-shifted emission peak (Fig. 4). This shift was attributed to the disruption of conjugation caused by the nitrogen atoms, leading to the formation of an intramolecular CT state as the lowest electronically excited state. Solvatochromic measurements of **CZ-ArB-5** revealed negative solvatochromism in absorption and positive solvatochromism in emission, indicating a solvent-dependent change in the compounds electronic properties. Despite these effects, the fluorescence quantum efficiency remained high in both solution and solid states. Cyclic voltammetry (CV) measurements revealed that both **CZ-ArB-4** and **CZ-ArB-5** experienced

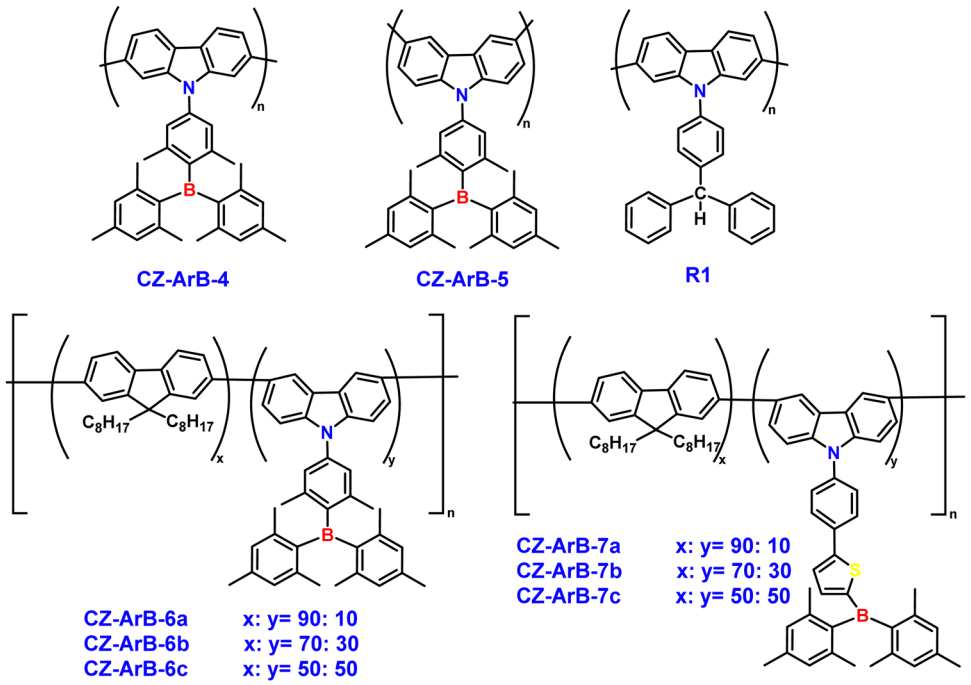

Fig. 3 Structure of compounds **CZ-ArB-4–7c**.

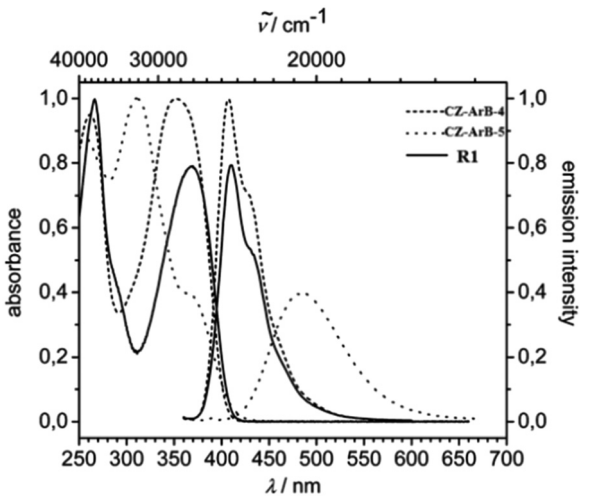

Fig. 4 Normalized absorption and emission spectra of **CZ-ArB-4-5** and **R1** in dichloromethane. Reproduced with permission from ref. 103. Copyright 2008 ACS.

cross-linking upon oxidation, producing two reversible oxidation peaks, unlike the reference polymer **R1**. Furthermore, the reduction process at the borane site was reversible in both **CZ-ArB-4** and **CZ-ArB-5**, while irreversible in **R1**. This cross-linking resulted in an increase in the HOMO levels of both **CZ-ArB-4** and **R1**, bringing them closer to those of 3,6-linked polycarbazoles. However, the LUMO energy levels of **CZ-ArB-4** were minimally affected by the cross-linking. Polymer **CZ-ArB-5**, which had an average polymerization degree of 12, demonstrated strong potential for OLED applications. It exhibited good solubility in common organic solvents, emitted blue light with high quantum efficiency, and showed excellent hole and electron transport properties. The CIE coordinates of (0.17, 0.21) further confirmed its suitability for efficient blue light emission in OLED devices. Following the above report, Jeng *et al.* developed a new class of carbazole/fluorene copolymers containing dimesitylboron side groups (**CZ-ArB-6a–c** and **CZ-ArB-7a–c**) using Suzuki coupling in 2011 (Fig. 3).[103] These copolymers demonstrated exceptional thermal stability, attributed to the incorporation of rigid carbazole–π–TAB units within the fluorene backbone. Compared to their fluorene homopolymer counterpart, poly(9,9-dioctylfluorene) (POF), the copolymers exhibited significantly enhanced photoluminescence (PL) quantum yields. This improvement underscores the synergistic interaction between the carbazole–π–boron side groups and the fluorene backbone. Electroluminescent (EL) devices fabricated using these copolymers showcased remarkable advancements in brightness and current efficiency. These enhancements were primarily driven by dual emission originating from both the fluorene backbone and the carbazole–π–boron side groups, coupled with reduced chain aggregation due to the structural rigidity imparted by the dimesitylboron units. Notably, the thiophene-linked **CZ-ArB-7a–c** unit exhibited a longer effective conjugation length compared to the phenyl-linked **CZ-ArB-6a–c** unit. This extended conjugation resulted in superior fluorescence properties for the thiophene-based polymers, demonstrating their advantage in device performance.

Wong *et al.* introduced a novel bipolar host material (**CZ-ArB-8**) incorporating dimesityl borane and carbazole, demonstrating high triplet energy and exceptional electroluminescent properties for phosphorescent OLEDs in 2011 (Fig. 7).[104] The

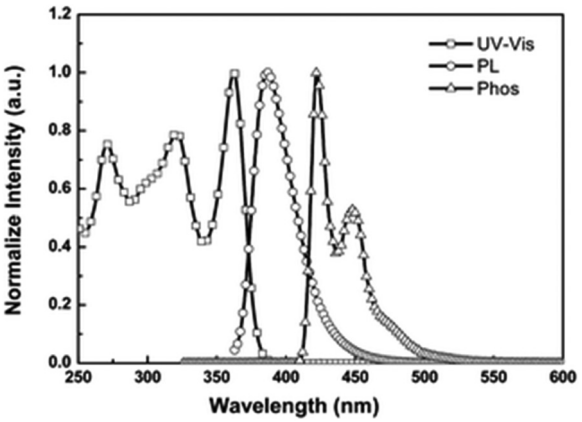

Fig. 5 UV-vis absorption, fluorescence spectra of **CZ-ArB-8** in DCM solution and the phosphorescence spectra at 77 K in EtOH. Reproduced with permission from ref. 104. Copyright 2012 Royal Society of Chemistry.

synthesis involved reacting 3,6-dibromo-*N*-phenyl carbazole with *n*-butyllithium, followed by quenching with fluorodimesitylborane, leading to the formation of the compound **CZ-ArB-8**. The absorption bands of compounds displayed at 271 nm, 321 nm, and 362 nm, with an emission peak at 386 nm and a triplet energy of 2.94 eV, which could be sufficient for red, green, blue, and white OLEDs device fabrication (Fig. 5). The compound **CZ-ArB-8** displayed bright luminescence and measured as 0.44 of PL quantum yield in CH_2Cl_2. The high triplet energy indicates the disruption of π-conjugation between the carbazole core and the mesityl rings *via* the boron atom, which leads to a highly twisted conformation. The compound's bipolar electrochemical properties and high glass transition temperature (T_g) make it a promising host for phosphorescent OLEDs across a wide color range. OLEDs fabricated using **CZ-ArB-8** demonstrated high EQEs: 20.7% for red, 20.0% for green, 16.5% for blue, and 15.7% for white at practical brightness levels. This underscores the potential of the **CZ-ArB-8** as a highly promising candidate for RGBW OLED applications, both in displays and lighting.

In 2012, Dong *et al.* introduced a novel A–π–D–π–A compound **CZ-ArB-9**, which features a large π-conjugated system with two dimesitylboron groups as electron acceptors and a carbazole dimer as the electron donor (Fig. 7).[105] The synthesis of compound **CZ-ArB-9** involved four steps: first, ethylation of carbazole, followed by a Vilsmeier–Haack reaction to form 9-ethylcarbazole-3-carbaldehyde. Then, 6-bromo-9-ethylcarbazole-3-carbaldehyde was prepared using NBS. A McMurry coupling was performed to yield (*E*)-1,2-bis(3-bromo-9-ethylcarbazol-6-yl)ethene, which was finally treated with ^{t}BuLi followed by addition of dimesitylboron fluoride to obtain the desired product **CZ-ArB-9**. The absorption spectra of **CZ-ArB-9** reveal two distinct bands: a π–π* transition (340–350 nm) and a broad ICT band (390–420 nm), attributed to the electron-donor carbazole core and electron-acceptor boron groups. Notably, **CZ-ArB-9** exhibits solvatochromism (Fig. 6(a)). Fluorescence titration studies show that **CZ-ArB-9** is highly sensitive to fluoride anions (F^-), with a distinct fluorescence "turn-off" at 500 nm and "turn-on" at 420 nm (Fig. 6(b)). This behavior is attributed to the transformation of the boron center from an electron-acceptor to an electron-donor, effectively disrupting the ICT process. Notably, the fluorescence response of **CZ-ArB-9** to F^- remains highly selective and unaffected by the presence of coexisting anions, highlighting its exceptional specificity. Theoretical calculations align closely with experimental observations, reinforcing the design of **CZ-ArB-9** as a promising candidate for advanced optoelectronic applications, including OLEDs, and for ratiometric fluorescence sensing. Following this, authors have developed two novel boron-based carbazole derivatives, **CZ-ArB-10a** and **CZ-ArB-10b**, featuring a D–π–A architecture with dimesitylboron acceptors and a 1,4-bis(carbazol-9-yl)benzene donor core, were developed to explore the impact of structural modifications on photophysical properties (Fig. 7).[106] **CZ-ArB-10a** exhibits unique photophysical properties, with its absorption maxima (350–360 nm) remaining stable across various solvents, while its fluorescence undergoes significant shifts based on solvent polarity. In THF–water mixtures containing more than 40% water, **CZ-ArB-10a**

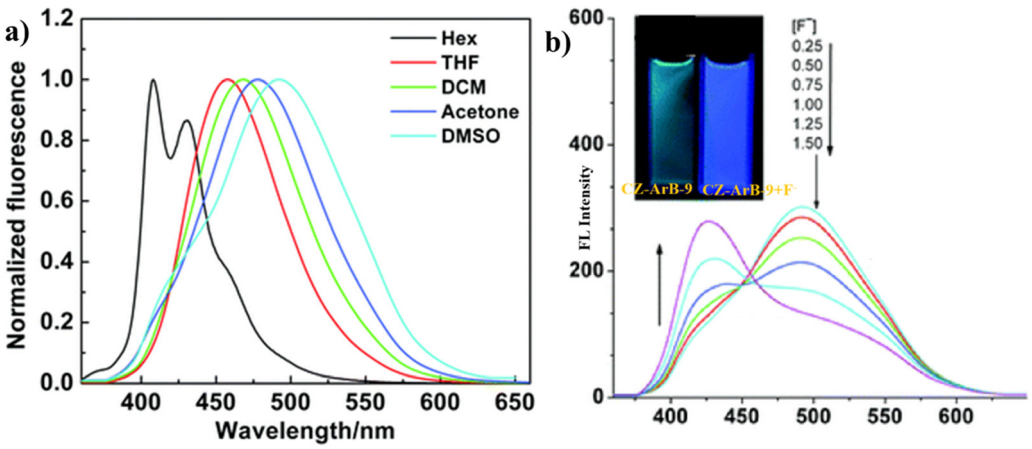

Fig. 6 (a) Fluorescence spectra of **CZ-ArB-9** with varying polarity of solvents. (b) Fluorescence titration spectra of **CZ-ArB-9** in DMSO upon gradual addition of F^-. Reproduced with permission from ref. 105. Copyright 2012 Royal Society of Chemistry.

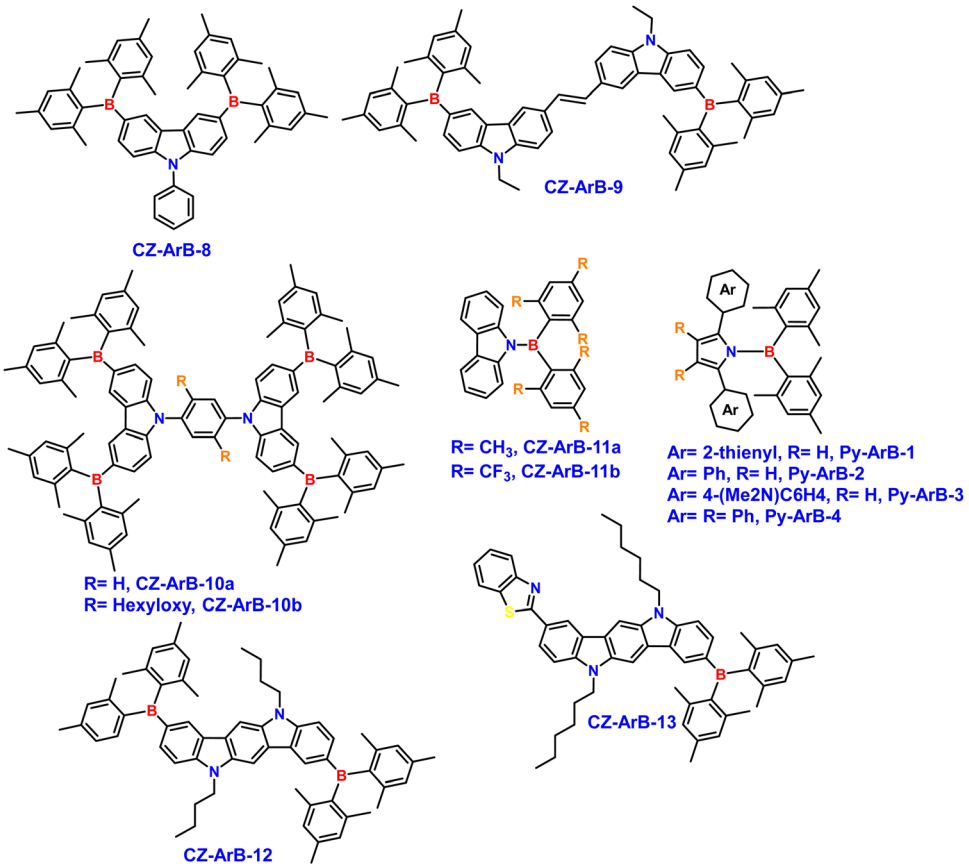

Fig. 7 Structure of compounds **CZ-ArB-8–13**.

self-assembles into nanoparticles, resulting in a dramatic fluorescence change from blue (395 nm) to green (485 nm). This process enhances the quantum yield from 0.23 to 0.36, attributed to aggregation-induced suppression of nonradiative decay pathways. Interestingly, these nanoparticles demonstrate vapor-responsive behavior, where exposure to chloroform vapor reversibly alters their fluorescence, shifting it from green back to sapphire blue. In comparison, the structural variant **CZ-ArB-10b**, featuring hexyloxy substituents, exhibits distinct behavior. The bulky hexyloxy groups introduce steric effects that inhibit AIE, leading to weak fluorescence in nanoparticle form. Unlike **CZ-ArB-10a**, **CZ-ArB-10b** fails to achieve the same level of donor–acceptor interaction, preventing the formation of tightly packed aggregates required for enhanced emission. The contrasting behaviors of **CZ-ArB-10a** and **CZ-ArB-10b** highlight the critical influence of molecular design on optical properties, aggregation tendencies, and environmental adaptability.

Liu *et al.* conducted an in-depth computational study on the electronic properties of 2,7- and 3,6-linked carbazole oligomers and their triarylborane-functionalized derivatives.[107] Utilizing density functional theory (DFT) and time-dependent DFT (TD-DFT) with long-range-corrected functionals, such as CAM-B3LYP and ωB97X, the study focused on how linkage topology and oligomer length influence charge transfer and excitation behavior. For 3,6-linked oligomers, the lowest excited state consistently involved ICT from the carbazole backbone to the electron-deficient triarylborane side chains. Conversely, in 2,7-linked systems, a shift was observed with increasing polymer length. While shorter oligomers exhibited similar ICT behavior, longer chains transitioned to a backbone-localized π–π* excitation as the dominant excited state. This transition reflected the extended conjugation inherent to the 2,7-linkage and was accurately described only with long-range-corrected functionals. Yamaguchi *et al.* introduced two novel carbazole derivatives, **CZ-ArB-11a** and **CZ-ArB-11b**, incorporating dimesitylboron groups with –OMe and $-CF_3$ substituents, respectively, to investigate the influence of functional groups on their photophysical properties (Fig. 7).[108] The study compared these derivatives with *N*-borylated 2,5-diarylpyrroles, shedding light on how substituents affect emission characteristics and solvent-dependent behavior. The methyl-substituted carbazole derivative **CZ-ArB-11a** exhibited absorption and emission maxima at 320 nm and 439 nm, respectively, in cyclohexane, with a Stokes shift of 8500 cm^{-1}, which, although smaller than the 13 500 cm^{-1} observed for Ph_2NBMeS_2, positions **CZ-ArB-11a** among compounds exhibiting TICT emissions. On the other hand, substituting the boron group with the highly electron-withdrawing $[2,4,6\text{-}(CF_3)_3C_6H_2]_2B$ in **CZ-ArB-11b** resulted in a significant redshift, with emission peaking at

603 nm over 160 nm longer than **CZ-ArB-11a**. This change was accompanied by a larger Stokes shift of 10 500 cm^{-1}, although the fluorescence quantum efficiency was lower compared to **CZ-ArB-11a**.

3.2. Indolocarbazole–triarylborane hybrids

Indolocarbazole–triarylborane hybrids represent a key subclass of D–A materials, combining the rigidity and planarity of indolocarbazole with the electron-accepting nature of triarylborane. These systems have shown enhanced conjugation and photophysical stability, making them promising candidates for high-performance optoelectronic devices. Dong *et al.* advanced their work by synthesizing a novel indolo[3,2-*b*]carbazole derivative featuring –$B(Mes)_2$ groups (**CZ-ArB-12**), marking the first report on such a boron-containing indolo[3,2-*b*]carbazole derivative (Fig. 7) in 2013.[109] The synthesis of the compound involved three steps, initially, 2,8-dibromoindolo[3,2-*b*]carbazole was prepared as the core intermediate. This was followed by the introduction of butyl groups through a reaction with C_4H_9Br and NaH in THF, resulting in 2,8-dibromo-5,11-dibutylindolo[3,2-*b*]carbazole. The final step involved lithiation with ^{n}BuLi and subsequent reaction with fluorodimesitylborane to yield the target compound (**CZ-ArB-12**). The absorption spectra of **CZ-ArB-12** show three absorption bands, with a low-energy broad band at 370–440 nm attributed to ICT from the indolo[3,2-*b*]carbazole core to the dimesitylboron terminals. The OLED devices incorporating **CZ-ArB-12** as the active emissive material demonstrated notable performance with pure blue emission centered at 440 nm. The undoped device exhibited a turn-on voltage of 3.6 V, achieving a peak luminance of 1455 cd m^{-2} and a luminance efficiency of 0.52 cd A^{-1}. Upon doping the emissive layer with 1% **CZ-ArB-12**, the device performance significantly improved, yielding a maximum luminance of 5342 cd m^{-2} and an enhanced efficiency of 1.67 cd A^{-1}. **CZ-ArB-12** showcased exceptional material characteristics, including high thermal durability (decomposition temperature T_d = 290 °C, glass transition temperature T_g = 170 °C) and impressive photophysical properties with a fluorescence quantum yield of 76%. Building on their previous work, the research group synthesized compound **CZ-ArB-13** by modifying **CZ-ArB-12**. The new design incorporated benzothiazole moieties, known for their electron-accepting properties, at the 2-position of indolo[3,2-*b*]carbazole, while replacing the butyl chain with a hexyl chain (Fig. 7).[110] These structural modifications enhanced the electron-accepting capability of **CZ-ArB-13**, making it highly suitable for anion sensing applications. When varying concentrations of fluoride ions (F^-) were introduced to a 1.0 × 10^{-5} M solution of **CZ-ArB-13**, a notable optical response was observed. The green ICT emission at 505 nm progressively decreased in intensity, while a new blue emission peak at 440 nm emerged. This distinct spectral shift facilitated reliable detection of F^- ions, with a calculated detection limit of 1.07 × 10^{-5} M. The interaction between **CZ-ArB-13** and F^- was further analyzed using the 1 : 1 Benesi–Hildebrand equation, which yielded an association constant of 2.05 × 10^5 M^{-1}, highlighting the compound's strong affinity and sensitivity toward fluoride ions. A Job's plot confirmed a 1 : 1 binding stoichiometry between **CZ-ArB-13** and F^- ions (Fig. 8).

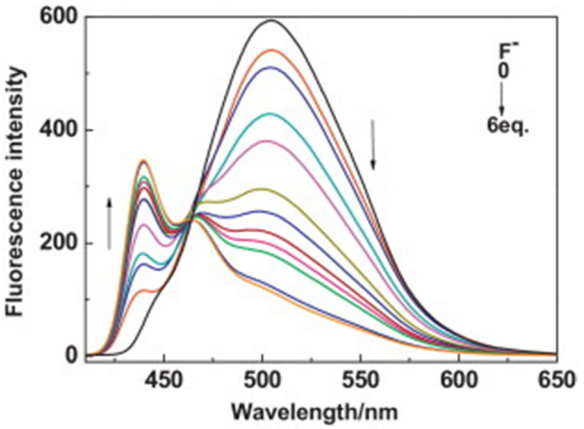

Fig. 8 Fluorescence titration spectra of **CZ-ArB-13** in DMSO upon addition of F^- ions. Reproduced with permission from ref. 110. Copyright 2013 Elsevier.

3.3. Mid-decade developments of carbazole triarylborane hybrids

In 2013, Wang *et al.* synthesized a novel carbazole derivative **CZ-ArB-14**, by introducing two dimesitylboron groups at the 3- and 3′-positions of 1,4-bis(carbazolyl)benzene (Fig. 11).[111] The compound **CZ-ArB-14** demonstrates excellent thermal stability (T_d = 190 °C) and electrochemical stability, along with AIE properties in THF/H_2O mixtures (Fig. 9(a)). A multi-layer electroluminescent device with **CZ-ArB-14** as the emitter delivered pure blue light (λ = 478 nm, CIE: 0.23, 0.35) with a turn-on voltage of 3.8 V, luminance efficiency of 3.25 cd A^{-1}, and maximum luminance of 2784 cd m^{-2}, showcasing its potential for efficient non-doped blue OLEDs. In parallel, Choi *et al.* designed an innovative star-shaped molecule, **CZ-ArB-15**, by attaching dimesitylboron groups to the 3,6-positions of carbazole and an additional dimesitylboron moiety to the 9-(4-phenyl) position.[112] This structural modification, absent in **CZ-ArB-8**, introduced enhanced electronic coupling and a more extended π-conjugation framework (Fig. 11). The synthesis involved a modified Ullmann reaction of 9*H*-carbazole with 4-bromoiodobenzene to form 9-(4-bromophenyl)-9*H*-carbazole, bromination with NBS to yield 3,6-dibromo-9-(4-bromophenyl)-9*H*-carbazole, and subsequent borylation using *t*-BuLi and dimesitylboron fluoride to produce **CZ-ArB-15**. The compound **CZ-ArB-15** displayed absorption bands at 290–330 nm (π–π* transitions) and 330–380 nm (ICT from carbazole to dimesitylboron), with an optical bandgap of 3.26 eV. The compound **CZ-ArB-15** displayed as strong fluorescence emission at 420 nm (ϕ_f = 0.95) and triplet energy of 2.83 eV highlighted its potential as a host for phosphorescent OLEDs (PhOLEDs) (Fig. 9(b)). **CZ-ArB-15** exhibited remarkable thermal endurance (T_d = 234 °C) and strong electrochemical resilience, establishing it as a promising host material for diverse PhOLED

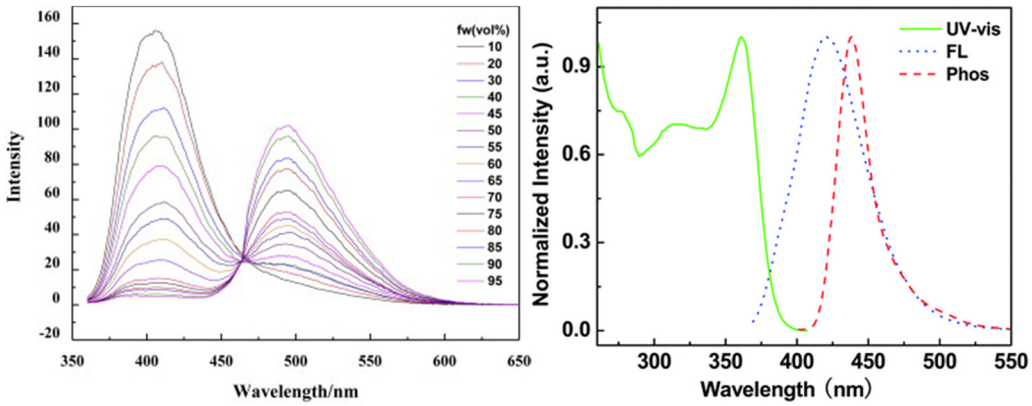

Fig. 9 Fluorescence spectra of **CZ-ArB-14** in the THF–water mixture with different fractions of water (f_w) (left). (UV-vis absorption, fluorescence) and phosphorescence spectra of **CZ-ArB-15** (right). Reproduced with permission from ref. 111 and 112 Copyright 2014 Elsevier, Royal Society of Chemistry.

applications. Red PhOLEDs utilizing $Os(bpftz)_2(PPh_2Me)_2$ as the dopant displayed a low operational threshold of 3.0 V, achieving a peak luminance of 12 337 cd m^{-2} and a commendable current efficiency of 11.04 cd A^{-1}. In green PhOLEDs with $Ir(ppy)_2(acac)$ as the dopant, the device delivered exceptional performance, including a turn-on voltage of just 2.5 V, an impressive maximum brightness of 26 473 cd m^{-2}, and an outstanding current efficiency of 38.60 cd A^{-1}. For blue PhOLEDs featuring FIrpic, **CZ-ArB-15** demonstrated its capability to support efficient emission, achieving a brightness of 7622 cd m^{-2} and a current efficiency of 7.39 cd A^{-1} at a turn-on voltage of 3.0 V.

In 2014, Hwang *et al.* reported the synthesis of two bipolar and high triplet energy phosphorescent host materials, **CZ-ArB-16** and **CZ-ArB-17**, which were designed by incorporating dimesitylborane and phenylcarbazole to investigate the effect of boron atom position on device performance (Fig. 11).[113] Compound **CZ-ArB-16** was synthesized by reacting 3-bromo-*N*-phenylcarbazole with ^{n}BuLi, followed by quenching with fluorodimesitylborane. Compound **CZ-ArB-17** was synthesized by *N*-arylation of 9*H*-carbazole with 1,4-dibromobenzene, followed by treatment with ^{n}BuLi and fluorodimesitylborane. Both compounds exhibited strong absorption peaks below 300 nm and an ICT band around 340 nm, corresponding to charge transfer from the carbazole to the TAB center. The photoluminescence emissions of **CZ-ArB-16** and **CZ-ArB-17** were observed at 400 nm and 430 nm, respectively. **CZ-ArB-17** displayed a 30 nm longer emission wavelength compared to **CZ-ArB-16**, with triplet energies of 2.88 eV and 2.72 eV for **CZ-ArB-16** and **CZ-ArB-17**, respectively, making both compounds suitable for use as green phosphorescent dopants (Fig. 10). Devices employing **CZ-ArB-17** as the host material demonstrated remarkable advancements, achieving a peak quantum efficiency of 23.8%, with minimal roll-off, maintaining 21.7% even at high luminance levels of 1000 cd m^{-2}. In comparison, devices based on **CZ-ArB-16** displayed a much lower efficiency of 6.5%. The enhanced performance of **CZ-ArB-17** is attributed to its balanced charge transport characteristics, efficient exciton generation, and suppression of non-radiative decay pathways.

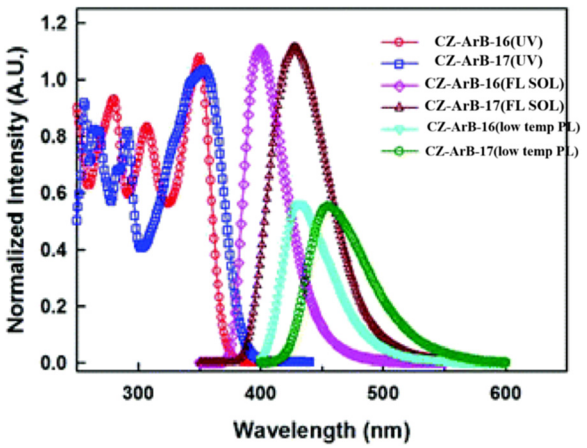

Fig. 10 UV/vis, solution PL and low temp. PL spectra of **CZ-ArB-16** and **CZ-ArB-17**. Reproduced with permission from ref. 113. Copyright 2014 Royal Society of Chemistry.

Kitamura *et al.* introduced two novel carbazole–triarylboranes derivatives, **CZ-ArB-18** and **CZ-ArB-19**, where the carbazole units were directly linked to triarylborane cores featuring xylene and anthracene frameworks, respectively (Fig. 11).[114] These compounds were designed to investigate the interplay between structural rigidity and electronic properties on their photophysical behavior. The triarylborane cores acted as electron-accepting centers, while the carbazole moieties served as electron donors, resulting in a donor–acceptor architecture. This configuration enabled effective ICT, which could be finely tuned by modifying the triarylborane substituents. **CZ-ArB-18**, with a more flexible xylene-based core, exhibited moderate charge transfer and a strong dependence on solvent polarity, leading to notable solvatochromic effects. In contrast, **CZ-ArB-19**, featuring a rigid anthracene-based core, displayed enhanced ICT efficiency, red-shifted emission, and higher photoluminescence quantum yields due to its more extended conjugation and reduced non-radiative decay. The optical properties of these compounds were further distinguished by their absorption profiles, with **CZ-ArB-18** showing a broader

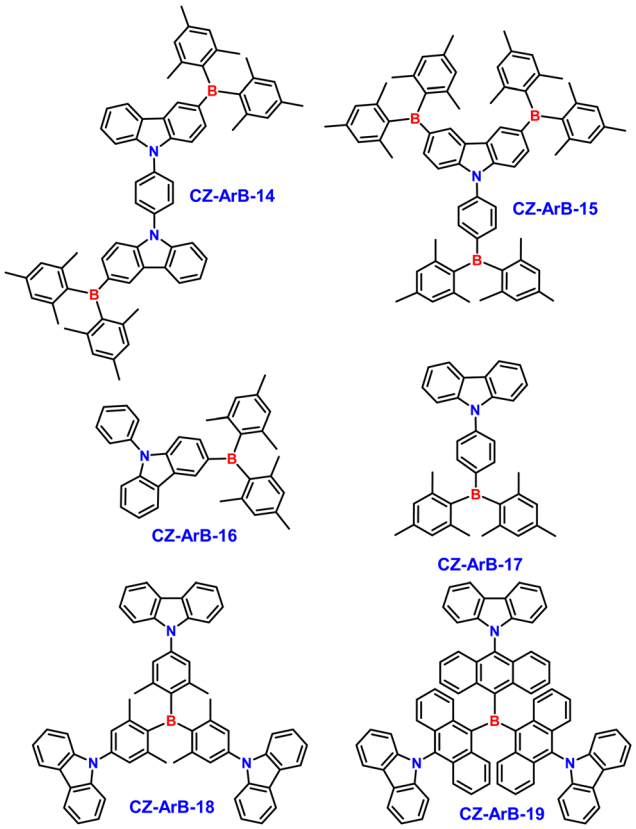

Fig. 11 Structure of compounds **CZ-ArB-14–19**.

absorption band, indicative of less restricted molecular vibrations, while **CZ-ArB-19** exhibited sharper absorption peaks consistent with its rigid structure. Electrochemical analysis revealed that both derivatives maintained excellent thermal and oxidative stability, making them promising candidates for optoelectronic applications.

Cheng *et al.* advanced their work by synthesizing two novel indolo[3,2-*b*]carbazole derivatives, **CZ-ArB-20** and **CZ-ArB-21**, by integrating one or two dimesitylboron groups into the indolo[3,2-*b*]carbazole backbone (Fig. 12).[115] **CZ-ArB-20** and **CZ-ArB-21** demonstrate exceptional optoelectronic properties attributed to their well-engineered molecular structures. Their

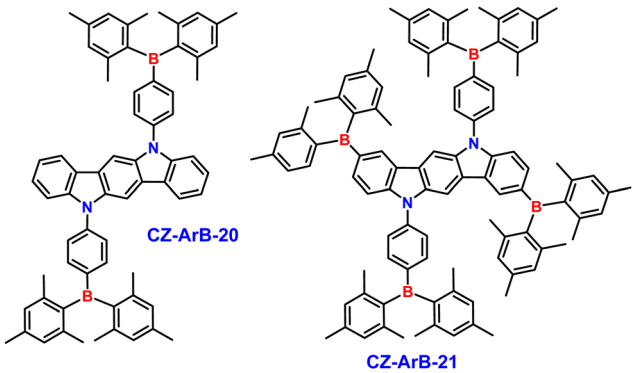

Fig. 12 Structure of compounds **CZ-ArB-20-21**.

emission spectra exhibited a substantial bathochromic shift across solvents, with λ_{em} transitioning from 425 nm in non-polar hexane to 540 nm in polar DMSO, confirming their significant solvent-polarity sensitivity and ICT dominance. Thermally, both compounds showed robust stability with decomposition temperatures exceeding 200 °C (T_d = 201 °C for **CZ-ArB-20** and 210 °C for **CZ-ArB-21**) and high glass transition temperatures (T_g = 145 °C and 162 °C, respectively). Their electrochemical profiles revealed reversible redox behavior and efficient charge-transport capabilities, reinforcing their suitability for electron-transport layers. In OLED device evaluations, **CZ-ArB-20** and **CZ-ArB-21** exhibited distinct performance metrics. **CZ-ArB-20**-based devices achieved a maximum luminance of 5634 cd m^{-2} with a luminance efficiency of 2.96 cd A^{-1}, though requiring a higher turn-on voltage of 6.1 V. Conversely, **CZ-ArB-21**-based devices displayed enhanced charge injection properties, evidenced by a reduced turn-on voltage of 3.6 V, while achieving a peak luminance of 1363 cd m^{-2} and a comparable luminance efficiency of 2.88 cd A^{-1}.

3.4. Tetraphenylethene (TPE)-based aggregation-induced emission (AIE) in carbazole–triarylboranes hybrids

Tetraphenylethene (TPE)-based aggregation-induced emission (AIE) plays a key role in enhancing the optoelectronic properties of carbazole–triarylborane hybrids. The incorporation of TPE into these systems significantly improves their solid-state fluorescence, making them ideal candidates for various applications such as sensing and high-performance OLEDs. Choi *et al.* developed a novel blue light-emitting **CZ-ArB-22**, this was the first report by combining tetraphenylethene (TPE) as an AIEE group, carbazole as a hole-transporting unit, and dimesitylboron as an electron-transporting group in 2014 (Fig. 13).[116] The synthesis of **CZ-ArB-22** involved multiple steps, starting with the creation of a key intermediate, 3-bromo-9-(4-(1,2,2-triphenylvinyl)phenyl)carbazole, using a modified Ullmann reaction. This intermediate was then reacted with ^{n}BuLi and dimesitylboron fluoride to yield the **CZ-ArB-22**. In THF/H_2O solvent systems, **CZ-ArB-22** demonstrated significant AIEE. The photoluminescence intensity at 475 nm showed an incredible increase of 256-fold, attributed to the restriction of intramolecular motions and enhanced radiative decay in the aggregated state (Fig. 14(a)). The electroluminescent properties of **CZ-ArB-22** were carefully examined, revealing a vivid blue emission centered at 464 nm, with CIE coordinates of (0.18, 0.21) across a range of applied voltages. When integrated into an OLED device, **CZ-ArB-22** exhibited a turn-on voltage of 6.0 V, achieving a maximum luminance of 4624 cd m^{-2} and a luminance efficiency of 4.28 cd A^{-1}. Tang *et al.* introduced the compound **CZ-ArB-23** (Fig. 13), featuring a tetraphenylethene (TPE) core integrated with carbazole for hole transport and a more robust dimesitylboron structure, containing double the boron units of its predecessor, **CZ-ArB-22**. This novel configuration resulted in remarkable photophysical properties. **CZ-ArB-23**[117] demonstrated excellent thermal stability with a decomposition temperature of 219 °C and superior electrochemical properties. The compound exhibited AIE behavior when

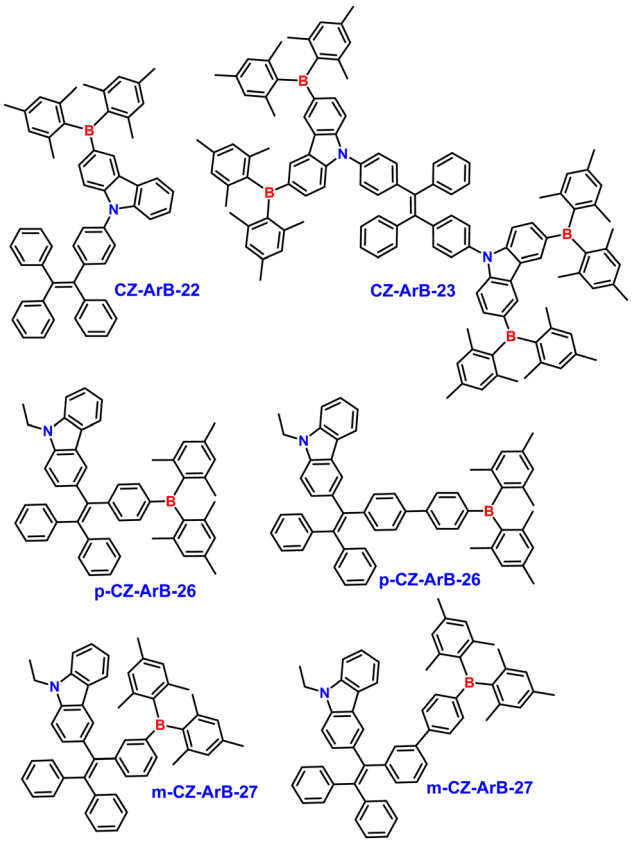

Fig. 13 Structure of compounds **CZ-ArB-22–27**.

dispersed in THF/H_2O mixtures, further enhancing its suitability for applications in OLEDs (Fig. 14(b)). In non-doped OLED devices, **CZ-ArB-23** delivered bluish-green light at 493 nm, with CIE coordinates of (0.19, 0.34). These devices achieved a low turn-on voltage of 5.2 V, a maximum luminance of 5406 cd m^{-2}, and a luminance efficiency of 5.34 cd A^{-1}.

Tang *et al.* pioneered further developments by synthesizing four novel AIE-active emitters ***p*-CZ-ArB-26**, ***m*-CZ-ArB-26**, ***p*-CZ-ArB-27**, and ***m*-CZ-ArB-27** featuring a triphenylethene–carbazole scaffold (Fig. 13).[118] These emitters were strategically designed by attaching an *N*-ethyl-carbazole unit to the 4-position of the TPE core. The *para* or *meta*-positions of the 3-phenyl group of TPE were functionalized with either dimesitylboron or (dimesitylboranyl)phenyl groups. The compounds were synthesized *via* Friedel–Crafts alkylation followed by Suzuki cross-coupling reactions. The compounds demonstrated remarkable thermal and morphological stability. The decomposition temperatures (T_d) were measured at 301 °C and 274 °C for ***p*-CZ-ArB-26** and ***p*-CZ-ArB-27**, respectively, while ***m*-CZ-ArB-26** and ***m*-CZ-ArB-27** exhibited even higher T_d values of 328 °C and 365 °C. Additionally, their high glass transition temperatures (T_g) of 100 °C, 115 °C, 138 °C, and 146 °C, respectively, highlight the robustness of their rigid aromatic frameworks, contributing to their excellent stability and structural integrity. The absorption spectra of ***p*-CZ-ArB-26** and ***m*-CZ-ArB-26** show three bands, including the TPE π–π* transition (~300 nm), carbazole π–π* (~330 nm), and ICT (~360 nm), while ***p*-CZ-ArB-27** and ***m*-CZ-ArB-27** exhibit blue-shifted ICT bands merging with the π–π* transition, indicating weaker donor–acceptor interactions. The *para*-linked compounds show stronger ICT effects than the *meta*-linked ones, with *m*-DBPDECZ exhibiting minimal or no clear ICT absorption. All compounds demonstrated AIE behavior in THF/H_2O mixtures, with emission properties tunable by linkage mode and conjugation length. The solid-state fluorescence quantum yields (ϕ values) of ***p*-CZ-ArB-26**, ***p*-CZ-ArB-27**, ***m*-CZ-ArB-26**, and ***m*-CZ-ArB-27** are calculated to be 99.3%, 48.6%, 34.6%, and 65.2%, respectively. Devices incorporating ***p*-CZ-ArB-26** and ***p*-CZ-ArB-27** exhibit maximum external quantum efficiencies of 2.73% and 3.28%, respectively, among the highest for non-doped green fluorescent devices at the time. In contrast, devices with *meta*-linked structures, such as ***m*-CZ-ArB-26** and ***m*-CZ-ArB-27**, display blue-shifted emissions due to their more twisted and less efficient conjugation. ***m*-CZ-ArB-26** turn on at 4.90 V, achieving 500 cd m^{-2} at 7.20 V and a peak luminance of 14 980 cd m^{-2} at 15 V, with a current efficiency of 2.53 cd A^{-1}, whereas ***m*-CZ-ArB-27**, with a turn-on voltage of 6 V, reaches a maximum current efficiency of 4.49 cd A^{-1} and a peak

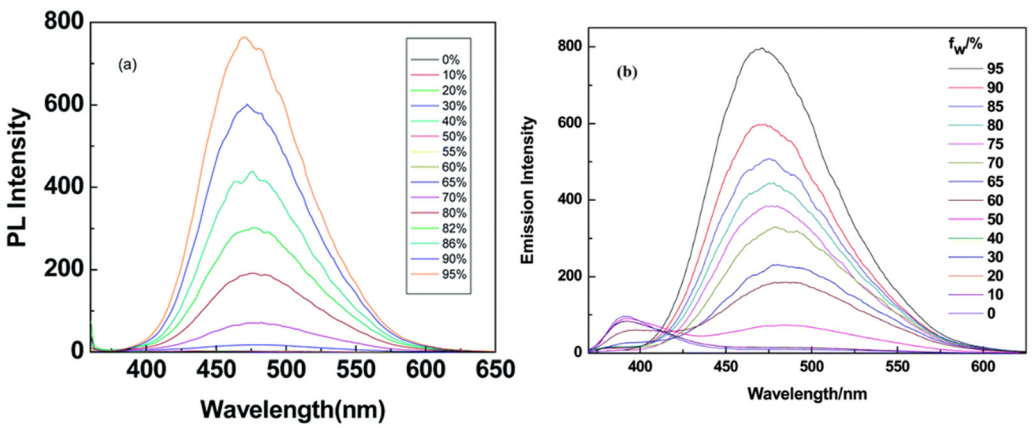

Fig. 14 PL spectra of (a) **CZ-ArB-22** and (b) **CZ-ArB-23** in various water contents of THF–water mixtures. Reproduced with permission from ref. 116 and 117. Copyright 2014, 2015 Royal Society of Chemistry.

luminance of 16 410 cd m^{-2}. From the same group synthesized two novel derivatives, **CZ-ArB-28** and **CZ-ArB-29**, by introducing dimesitylboron and tetraphenylethene at the 3,6-positions of carbazole, unlike the 9th-position substitutions in **CZ-ArB-22** and **CZ-ArB-23** (Fig. 18).[119] The multi-step synthesis began with Friedel–Crafts acylation of 3-bromo-9-ethyl-9*H*-carbazole, followed by treatment with lithiated diphenylmethane and acidic dehydration to yield 3-bromo-9-ethyl-6-(1,2,2-triphenylvinyl)-9*H*-carbazole. The key intermediate was dimerized using a McMurry cross-coupling reaction, and final lithiation with ^{n}BuLi, followed by dimesitylboron fluoride substitution, yielded **CZ-ArB-28** and **CZ-ArB-29**. The compounds exhibit excellent thermal stability (T_d up to 254 °C), along with high electrochemical stability, solid-state emission, and AIE properties. Additionally, multi-layer electroluminescent devices incorporating **CZ-ArB-28** and/or **CZ-ArB-29** as the light-emitting layer were fabricated, resulting in sky blue and blue-green emissions. These devices achieved maximum luminance efficiencies of up to 6.90 cd A^{-1} and maximum luminance values of 15 780 cd m^{-2}, with CIE of (0.20, 0.28) and (0.23, 0.41), respectively. In continuation, they introduced another novel derivative, **CZ-ArB-30**, (Fig. 13)[120] with slight difference from the previous derivatives (**CZ-ArB-28** and **CZ-ArB-29**). The structure featured the incorporation of two dimesitylboron groups at the 3- and 6-positions and a tetraphenylethene group at the 9-position of carbazole. This design differs from **CZ-ArB-30** by the addition of a dimesitylboron group at the 6-position of the carbazole core. The thermal, electrochemical, and photophysical properties of compound **CZ-ArB-30** were characterized using TGA, electrochemistry, UV-vis absorption, and fluorescence spectroscopy. The results showed that **CZ-ArB-30** exhibits excellent AIE properties and good thermal stability (T_d = 173 °C). Furthermore, a multilayer EL device using **CZ-ArB-30** as the light-emitting layer was fabricated. The device emitted blue light (λ_{max} = 489 nm) with CIE coordinates of (0.17, 0.29), and demonstrated good electroluminescent performance, with a turn-on voltage of 5.7 V, maximum luminance of 5709 cd m^{-2} (at 15 V), and a maximum luminance efficiency of 4.31 cd A^{-1} (at 8.2 V) (Fig. 15).

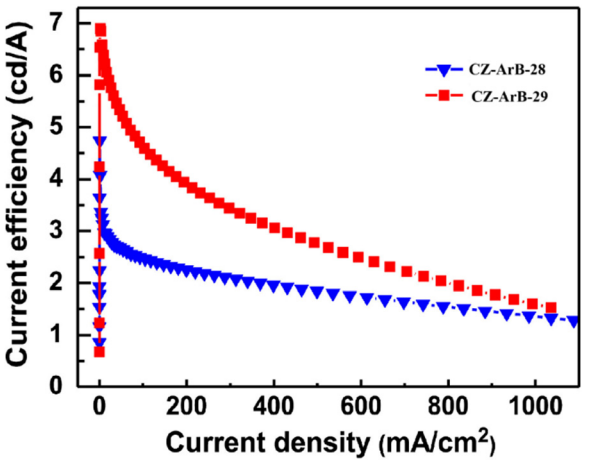

Fig. 15 Current efficiency *vs.* current density curves of device of **CZ-ArB-28** and **CZ-ArB-29**. Reproduced with permission from ref. 119. Copyright 2016 Elsevier.

Building on their previous work, researchers developed two novel compounds, **CZ-ArB-31** and **CZ-ArB-32** (Fig. 18),[121] by modifying the diphenylethene core of **CZ-ArB-28** and **CZ-ArB-29** with carbazole and dimesitylboron units. These modifications significantly enhanced the thermal and optical properties of the resulting compounds. Both **CZ-ArB-31** and **CZ-ArB-32** exhibited exceptional thermal stability, with decomposition temperatures (T_d) of 228 °C and 235 °C, respectively. This stability was attributed to the steric protection provided by the carbazole and dimesitylboron units, which also contributed to their robust structural rigidity, reflected in their glass transition temperatures (T_g) of 95 °C for **CZ-ArB-31** and 139 °C for **CZ-ArB-32**. The absorption spectra of both compounds were nearly identical, showing a sharp peak at 305 nm, which is attributed to the π–π* transitions within the molecular skeleton, and a broad band centered around 400 nm, corresponding to ICT from the electron-rich carbazole moiety to the electron-deficient dimesitylboron groups. In terms of luminescence, both compounds exhibited strong green emissions, with **CZ-ArB-31** emitting at 520 nm and **CZ-ArB-32** at 540 nm, the latter showing a red-shifted emission due to enhanced conjugation and stronger intermolecular interactions. In THF/H_2O mixtures, both compounds exhibited AIE behavior, further demonstrating their potential for optoelectronic applications (Fig. 16). OLED devices fabricated using **CZ-ArB-31** emitted yellowish-green light with a peak at 537 nm, a turn-on voltage of 3.8 V, a maximum brightness of 59 130 cd m^{-2}, and a maximum current efficiency of 6.43 cd A^{-1}. Devices made with **CZ-ArB-32** showed greenish-yellow light with a peak at 554 nm, a reduced turn-on voltage of 3.0 V, a maximum brightness of 67 500 cd m^{-2}, and an enhanced current efficiency of 11.2 cd A^{-1}.

Alongside, in 2017 they developed three novel compounds, **CZ-TAB-33** to **CZ-TAB-35**, characterized by a fused phenylvinylcarbazole core (Fig. 18).[122] The **CZ-TAB-33** structure is the modified version of **CZ-ArB-28** by incorporating a phenyl attached dimesitylboron unit. These compounds demonstrated thermal stability with decomposition temperatures (T_d) of 219 °C, 188 °C, and 167 °C for **CZ-ArB-33**, **CZ-ArB-34**, and **CZ-ArB-35**, respectively. These compounds, exhibiting typical AIE characteristics in THF/H_2O mixtures, (Fig. 17) demonstrated efficient solid-state emission and well-adjusted HOMO–LUMO energy levels, making them highly suitable for advanced OLED applications with enhanced performance and durability. The solid-state absolute quantum yields calculated for **CZ-ArB-33**, **CZ-ArB-34**, and **CZ-ArB-35**, are 55.6, 48.7, and 35.9%, respectively. Non-doped OLED devices were fabricated using **CZ-ArB-33**, **CZ-ArB-34**, and **CZ-ArB-35**, as emissive layers, producing distinct electroluminescent emissions. Compound **CZ-ArB-33** emitted blue-green light with a peak at 513 nm, while **CZ-ArB-34**, and **CZ-ArB-35** showcased deep blue and sky-blue emissions with peaks at 438 nm and 488 nm, respectively. The devices exhibited excellent performance metrics, including low turn-on

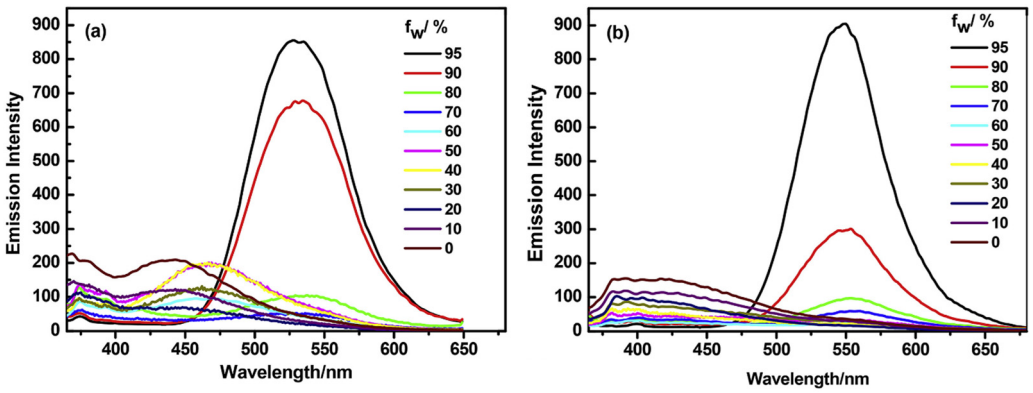

Fig. 16 Emission spectra of **Cz-ArB-31** (a) and **CZ-ArB-32** (b) in various water contents of THF–water mixtures (excitation wavelength = 330 nm and 350 nm, respectively). Reproduced with permission from ref. 121. Copyright 2016 Elsevier.

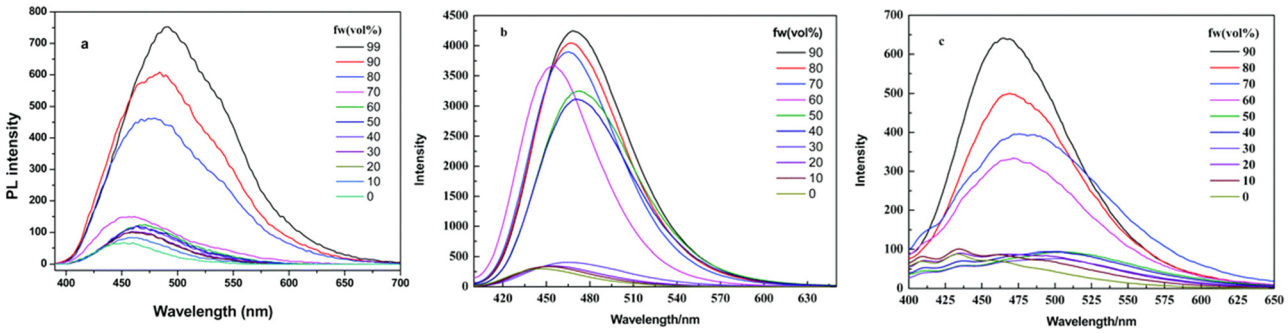

Fig. 17 PL spectra of (a) **CZ-ArB-33**, (b) **CZ-ArB-34** and (c) **CZ-ArB-35** in THF/water mixtures with various water fractions. Reproduced with permission from ref. 122. Copyright 2021 Royal Society of Chemistry.

voltages of 6.2 V, 6.0 V, and 6.3 V, alongside maximum brightness levels of 21 054 cd m^{-2}, 4376 cd m^{-2}, and 12 080 cd m^{-2} for **CZ-ArB-33**, **CZ-ArB-34**, and **CZ-ArB-35**, respectively. Maximum current efficiencies reached 3.34 cd A^{-1} for **CZ-ArB-33**, 2.34 cd A^{-1} for **CZ-ArB-34**, and 1.73 cd A^{-1} for **CZ-ArB-35**. Additionally, the devices exhibited operational stability with minimal efficiency roll-off, highlighting the robustness of the materials.

3.5. Recent advances and emerging trends of carbazole–triarylboranes hybrids (2015–2020)

In a significant advancement in the field of thermally activated delayed fluorescence (TADF), Kaji *et al.* developed two novel carbazole-based triarylborane emitters, **CZ-ArB-24** and **CZ-ArB-25**, in **2015** (Fig. 19).[123] These compounds were strategically designed by incorporating carbazole as the electron-donating unit, paired with a robust trimesitylborane core, to enhance charge transfer capabilities and minimize the singlet–triplet energy gap (ΔE_{ST}), which is crucial for efficient TADF. Both compounds exhibited remarkable photophysical properties, with **CZ-ArB-24** reaching an outstanding photoluminescence quantum yield of 100%, and **CZ-ArB-25** achieving 87% in a DPEPO host matrix. These high quantum yields reflect the compounds strong ability to radiative pathway efficiently, ensuring minimal energy losses due to non-radiative processes. When applied to OLEDs, **CZ-ArB-24** achieved a groundbreaking external quantum efficiency (η_{EQE}) of 21.6%, setting a new benchmark for sky-blue TADF-based OLEDs. **CZ-ArB-25** also demonstrated strong performance, with an EQE of 14.0%. These findings underscore the potential of these emitters for use in high-performance OLED devices, paving the way for the development of energy-efficient, durable, and vivid blue-emitting displays and lighting solutions. In 2017, Lee *et al.* synthesized and analyzed highly efficient TADF *ortho* donor–acceptor (D–A) compounds featuring triarylboron acceptors and phenoxazine (PXZ), diphenylamine (DPA), or carbazole (Cz) donors.[124] The *ortho*-connected carbazole–triarylboranes (**CZ-ArB-36**) (Fig. 23) was compared to its *para*-connected counterpart (**CZ-ArB-17**). The *ortho* D–A arrangement, combined with the bulky triarylboranes group, induces a sterically locked, highly twisted geometry, resulting in a small ΔE_{ST} and displayed as microsecond-range TADF lifetimes. In contrast, the *para* derivatives only exhibit short-lived fluorescence and does not show TADF ability. OLEDs incorporating *ortho* D–A compounds, such as **CZ-ArB-36**, demonstrated exceptional performance, achieving a high η_{EQE}. Notably, the pure blue emission OLEDs exhibited a η_{EQE} of 22.6%, which was further optimized to an impressive 24.1%. This remarkable enhancement

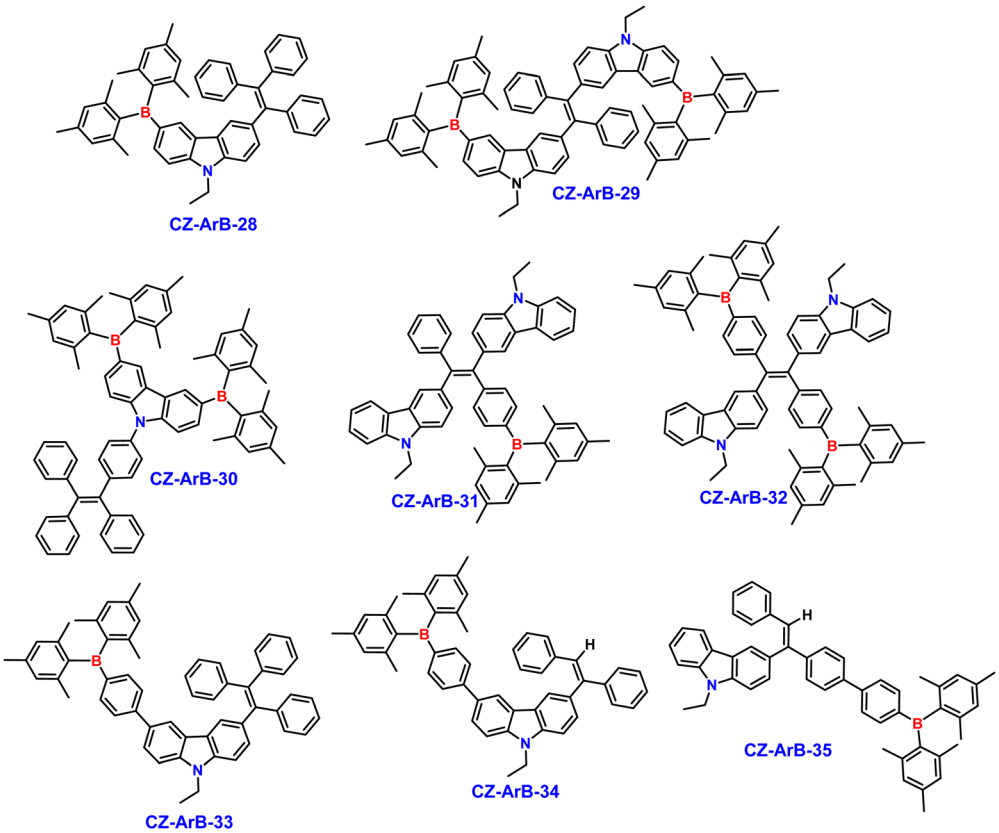

Fig. 18 Structure of compounds **CZ-ArB-28–35**.

underscores the potential of *ortho* D–A compound-based OLEDs for high-efficiency optoelectronic applications. Building on this, the following year, the authors developed a series of *ortho*-carbazole-appended triarylboranes compounds (**CZ-ArB-37a–e**) with varying substituents such as ^{t}Bu, Me, and OMe on the carbazole donor and/or phenylene ring of the dimesitylboron acceptor (Fig. 23).[125] These compounds were synthesized *via* a reaction between dimesitylboron fluoride and lithium salts of *ortho*-carbazole-substituted bromobenzenes, yielding products with strong ICT absorption bands (370–410 nm) and tunable emission from sky blue (481 nm) to ultradeep blue (438 nm). Substituent effects influenced the HOMO–LUMO levels, with ^{t}Bu inducing a bathochromic shift and OMe causing a hypsochromic shift. Emission properties correlated with ΔE_{ST} values, with ^{t}Bu and Me-substituted compounds (**CZ-ArB-37a** and **CZ-ArB-37b**) exhibiting smaller ΔE_{ST} (<0.1 eV) and higher photoluminescence quantum yields (PLQY) due to efficient TADF, compared to compounds **CZ-ArB-37c-e** (ΔE_{ST} = 0.15–0.16 eV). Blue OLEDs based on **CZ-ArB-37b** achieved a remarkable EQE of 32.8% at CIE (0.135, 0.266), attributed to its high PLQY (93%) and horizontal transition dipole ratio (0.76). Ultradeep blue OLEDs using **CZ-ArB-37e** also demonstrated a record-high EQE of 14.9% at CIE (0.151, 0.058).

Huang *et al.* synthesized four triarylborane-based compounds with symmetric and asymmetric architectures featuring carbazole and diphenylamine donor branches in 2018 (Fig. 19).[126] These compounds exhibited excellent thermal stability with high decomposition (T_d > 416 °C), glass-transition (T_g > 158 °C), and melting temperatures (T_m > 213 °C), attributed to the stabilized boron core and bulky peripheral groups. Asymmetric compounds (**CZ-ArB-38**, **CZ-ArB-40**) showed superior thermal properties compared to symmetric ones (**DP-ArB-2**, **CZ-ArB-39**), making them promising candidates for OLED host materials. The compounds exhibited distinct π–π* transitions (~295 nm) and weaker n–π* transitions (~340 nm), with their asymmetric architectures (**CZ-ArB-38**, **CZ-ArB-40**) displaying larger Stokes shifts and higher thermal and optical stability (Fig. 20). Optical bandgaps ranged from 3.30–3.45 eV, and triplet energy levels were high (2.77–2.90 eV), making them suitable as host materials for blue phosphorescent OLEDs (PhOLEDs). Devices based on asymmetric compounds (**CZ-ArB-38**, **CZ-ArB-40**) outperformed their symmetric counterparts (**DP-ArB-2**, **CZ-ArB-39**), with **CZ-ArB-40** achieving maximum EQE of 18.5%, current efficiencies (CE) of 38.9 cd A^{-1}, and power efficiencies (PE) of 30.5 lm W^{-1}, along with lower turn-on voltages (3.5 V).

In **2019**, Lu and colleagues developed two new bipolar host materials (**CZ-TAB-41** and **CZ-TAB-42**) combining carbazole and triarylborane units, designed with donor and acceptor groups positioned *meta* to each other on a central benzene ring (Fig. 21).[127] This spatially congested configuration enhances molecular compactness and significantly improves thermal stability. Both compounds exhibit weak blue-violet emission and high triplet energy levels of 2.68 eV for **CZ-TAB-41** and

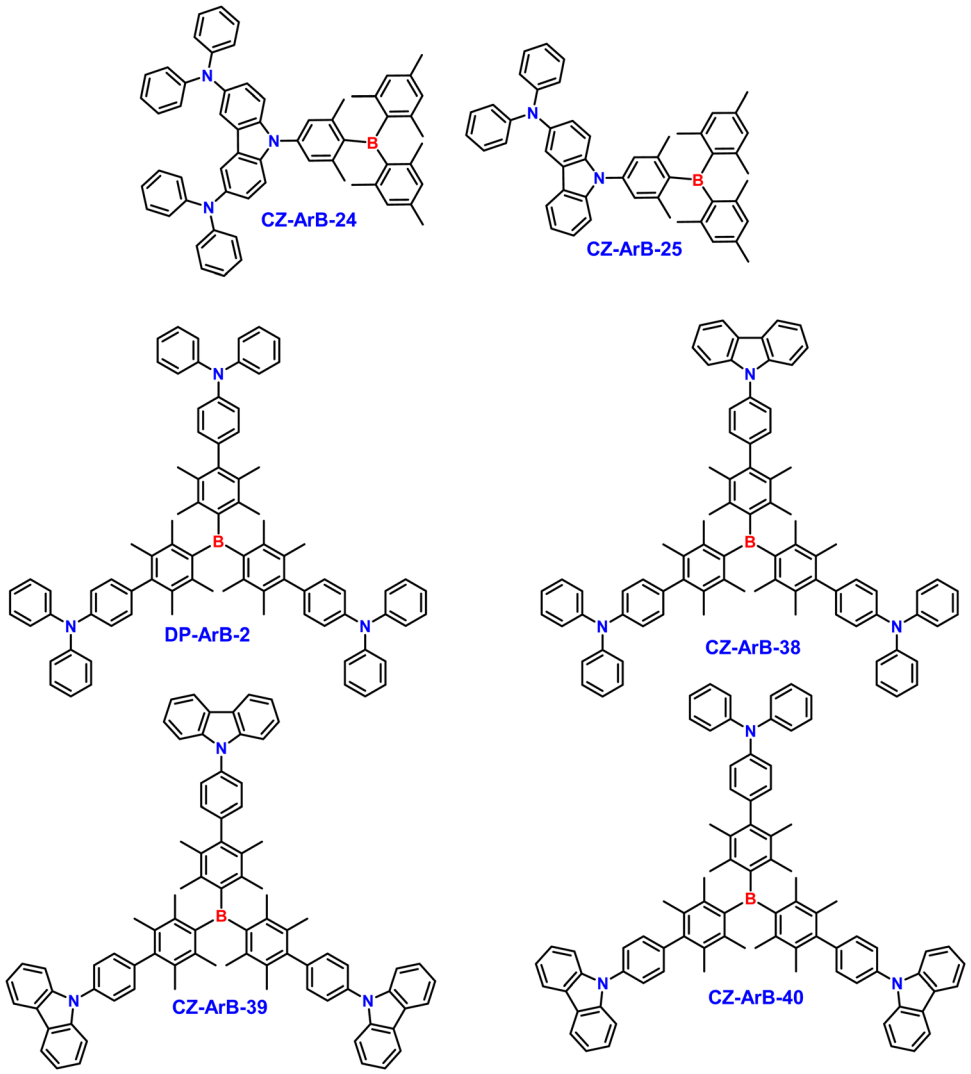

Fig. 19 Structure of compounds **Cz-ArB-24-25**, **DP-ArB-2** and **CZ-ArB-38–40**.

2.63 eV for **CZ-TAB-42**, suitable for hosting green phosphorescent emitters. The materials demonstrate excellent thermal stability, with decomposition temperatures exceeding 340 °C for **CZ-TAB-41** and 290 °C for **CZ-TAB-42**, attributed to their highly twisted molecular architecture. Phosphorescence peaks recorded at 77 K at 463 nm (**CZ-TAB-41**) and 472 nm (**CZ-TAB-42**) further confirm their suitability for energy transfer in green phosphorescent systems (Fig. 22). Green-emitting OLEDs utilizing $Ir(ppy)_3$ as the emitter and **CZ-TAB-41** or **CZ-TAB-42** as host materials achieved remarkable efficiencies. Devices featuring **CZ-TAB-41** exhibited a maximum EQE of 19.3%, a current efficiency of 69.1 cd A^{-1}, and a power efficiency of 88.1 lm W^{-1}, with a low turn-on voltage of 2.4 V. Similarly, devices with **CZ-TAB-42** achieved an EQE of 19.1%, a current efficiency of 66.1 cd A^{-1}, and a power efficiency of 77.2 lm W^{-1}, with a turn-on voltage of 2.6 V.

Later in 2019, Lee *et al.* synthesized a new series of *ortho*-carbazole-appended triarylborane compounds (**CZ-TAB-43a–f**) by introducing various electron-accepting substituents, including phenyl, pyridyl, pyrimidyl, diphenylphosphine oxide, cyano, and dimesitylboryl groups, on the phenylene ring of the triarylborane acceptor (Fig. 23).[128] Unlike the **CZ-ArB-37** series, the **CZ-ArB-43** series features substitution only at the 5th position of the 9-phenyl-substituted carbazole, rather than at the 3rd or 6th positions. These modifications allowed precise tuning of their photophysical properties. Emission spectra exhibited broad ICT-based bands, shifting from blue (463 nm) to greenish-yellow (532 nm), with PL quantum yields (Φ) ranging from 48% to 93% in oxygen-free toluene. Strong electron acceptors, such as diphenylphosphine oxide, cyano, and dimesitylboryl, significantly enhanced emission efficiency. Electrochemical and theoretical studies confirmed that red-shifted emissions resulted from stabilized LUMO levels and small ΔE_{ST}, enabling efficient TADF. From the same group, further refined the design by introducing strong electron-withdrawing perfluoro substituents, such as perfluoroalkyl (CF_3, C_3F_7) and perfluoroaryl (4-$CF_3C_6F_4$) groups, into the triarylborane acceptor moiety in 2020 (Fig. 23).[129] This

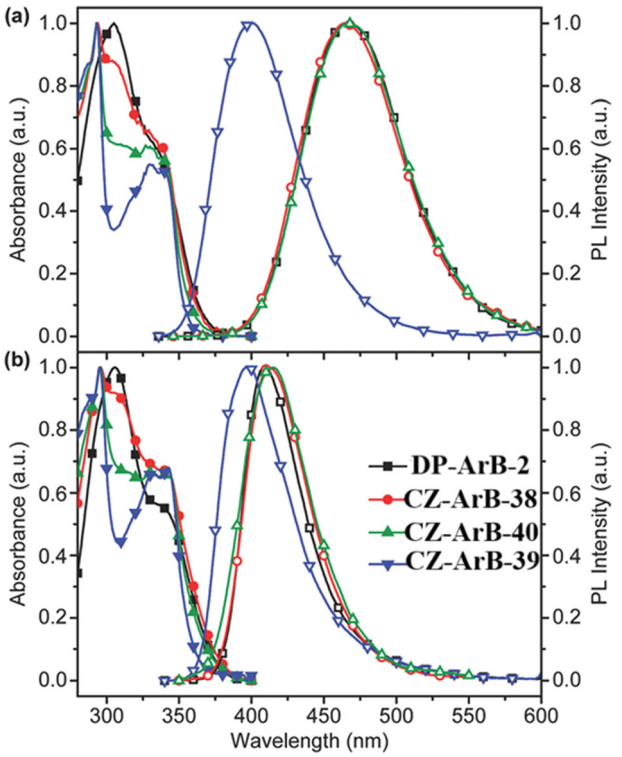

Fig. 20 UV-absorption (solid symbols) and emission spectra (open symbols) of **DP-ArB-2**, **CZ-ArB-38–40** in (a) DCM solution and (b) solid films. Reproduced with permission from ref. 126. Copyright 2018 Wiley.

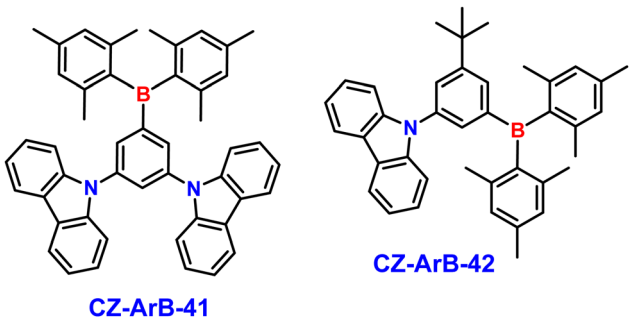

Fig. 21 Structure of compounds **CZ-ArB-41-42**.

structural evolution aimed to enhance the optoelectronic properties and further leverage the donor–acceptor framework for efficient TADF. These new compounds (**CZ-ArB-44a–f**) displayed green to yellow emission in toluene with exceptionally high PLQYs of up to 100%. The inclusion of perfluoro groups introduced greater electron-withdrawing character, which, coupled with the twisted D–A architecture confirmed by X-ray crystallography and computational studies, resulted in a small $\Delta E_{ST} < 0.1$ eV. In OLED applications, the CF_3- and 4-$CF_3C_6F_4$-substituted compounds proved to be excellent emitters, achieving high external quantum efficiencies of up to 29.9% (*e.g.*, **CZ-ArB-44d**) and a maximum PE of 123.9 lm W^{-1}—one of the highest values reported for TADF-OLEDs at that time. Importantly, these devices demonstrated stable performance at practical brightness levels, maintaining PEs of 118.7 lm W^{-1} at 100 cd m^{-2} and 82.3 lm W^{-1} at 1000 cd m^{-2}, while operating at a remarkably low turn-on voltage (V_{on}) of 2.35 V without the need for light outcoupling enhancements.

In **2020**, Chi and colleagues synthesized three methoxy-substituted carbazoles (**CZ-OMe-45a–c**) to enhance electron-donating strength.[130] These carbazole donors were coupled with a dimesitylboron acceptor to form compounds (**CZ-TAB-45a-b**) and phenylene-bridged emitters (**CZ-TAB-46a-b**) (Fig. 24). Comprehensive photophysical analysis in various solvents revealed a pronounced solvatochromic response, driven by strong charge transfer interactions within the molecular framework. In contrast to earlier analogs like **CZ-ArB-10a** and **CZ-ArB-17**, which lacked TADF behavior, the newly developed emitters displayed robust TADF, attributed to the strategic introduction of methoxy groups. When integrated into OLED devices, the emitters delivered blue emissions with peaks spanning from 444 nm to 468 nm. Notably, devices incorporating **CZ-ArB-45b** and **CZ-ArB-46b** demonstrated outstanding maximum EQE of 12.5% and 13.3%, respectively, showcasing their suitability as efficient blue-emitting materials for cutting-edge OLED applications.

In 2020, Marder *et al.* introduced a groundbreaking approach for designing efficient TADF emitters, utilizing computational strategies to refine excited state properties.[131] By developing an advanced theoretical model, they were able to describe both local and charge-transfer states and manipulate these states to control key processes such as ISC and rISC. Their innovative strategy involved adjusting the energy of the local excited state at the bridge (^{3}LEπ), which in turn influenced the relative stability of this state compared to charge-transfer states. Their theoretical predictions were experimentally validated through the synthesis of five D–A compounds featuring carbazole and phenoxazine. These compounds demonstrated a reduced singlet–triplet gap, which led to delayed fluorescence as anticipated, with emission wavelengths spanning from deep blue to red. In their proof of concept, Marder and team synthesized carbazole derivatives, **CZ-ArB-47a** and **CZ-ArB-47b** (Fig. 24), with different donor-bridge configurations. These compounds exhibited significant solvatochromism and displayed impressive TADF characteristics. **CZ-ArB-47a** showcased near-unity quantum yield and efficient fluorescence, while **CZ-ArB-47b**, with methyl group substitutions, increased the dihedral angle and enhanced charge-transfer properties. This structural modification led to a noticeable shift in emission characteristics, including delayed fluorescence. The study emphasized the importance of donor–acceptor interactions in determining photophysical properties, as evidenced by solvatochromic behavior and solvent-dependent quantum yields. This research paves the way for the computational design of highly efficient, tunable TADF emitters, opening new avenues for OLED applications.

In 2020, Tang and colleagues introduced a novel carbazole–triarylboranes derivative, **CZ-ArB-48** (Fig. 26).[132] This compound is a modified version of **CZ-ArB-41**, with an additional

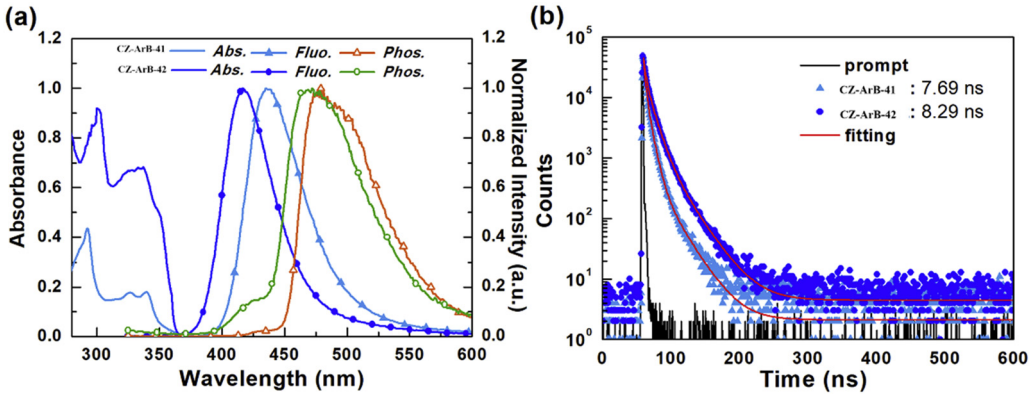

Fig. 22 (a) UV-vis absorption, fluorescence, and phosphorescence spectra of **CZ-ArB-41** and **CZ-ArB-42** in thin films. (b) Transient photoluminescence decay profiles of **CZ-ArB-41** and **CZ-ArB-42** thin films upon excitation at 365 nm. Reproduced with permission from ref. 127. Copyright 2019 Elsevier.

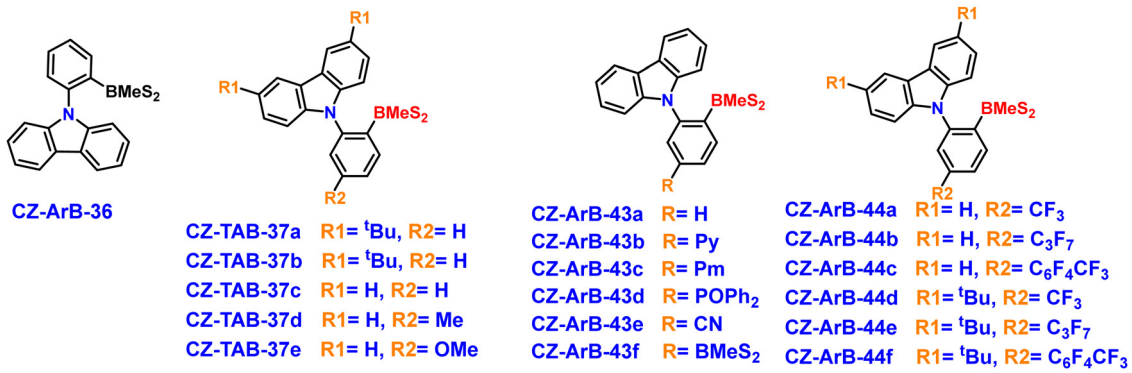

Fig. 23 Structure of compounds **CZ-ArB-36-37e**, **CZ-ArB-43a-6** and **CZ-ArB-44a–f**.

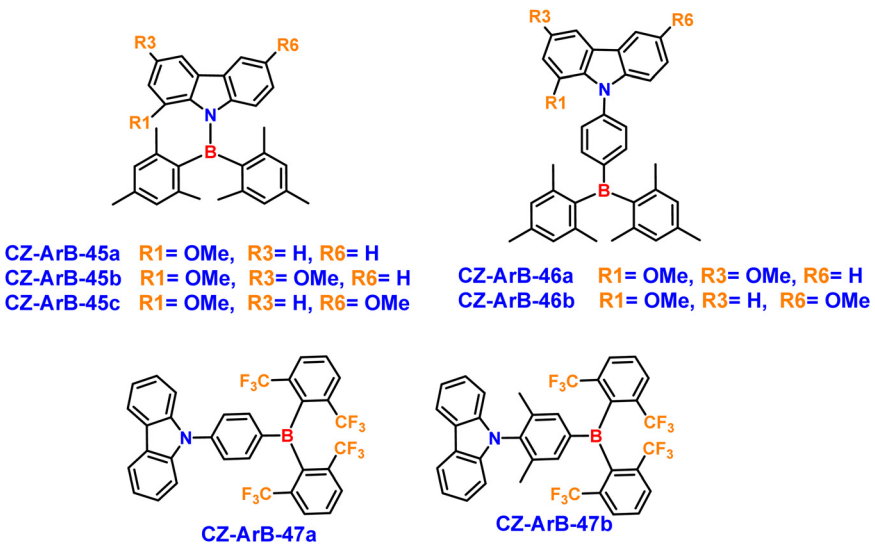

Fig. 24 Structure of compounds **CZ-ArB-45a–47b**.

phenyl ring attached to the triarylborane unit. The donor atom is positioned *meta* to the new phenyl ring, which results in an unusual structural configuration. **CZ-ArB-48** demonstrated exceptional thermal stability (T_d = 394 °C) and exhibited AIEE behavior (Fig. 25). The X-ray analysis revealed a monoclinic crystal structure with a twisted propeller configuration,

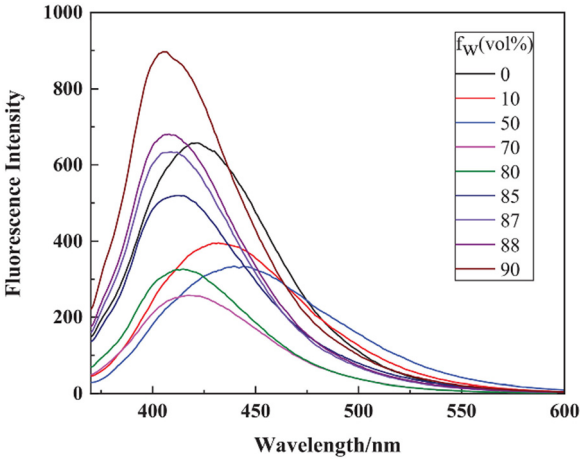

Fig. 25 Emission spectra of **CZ-ArB-48** in THF/water mixtures with different water fractions. Reproduced with permission from ref. 132. Copyright 2021 Elsevier.

stabilized by C–H···π and hydrogen bonding, but without π–π interactions, which are crucial for the AIEE effect. The OLEDs based on **CZ-ArB-48** emitted bluish-violet light at 425 nm, with a turn-on voltage of 5.6 V and a maximum luminance of 5374 cd m^{-2}. The devices showed peak efficiencies of 2.26 cd A^{-1} and 0.96 lm W^{-1}, with stable performance and minimal efficiency roll-off. In another study, Hong *et al.* synthesized two novel TADF emitters, **CZ-ArB-49** and **CZ-ArB-50** (Fig. 26), which incorporated triarylborane as the electron acceptor and carbazole-based donors, with phenoxazine replacing carbazole in **CZ-ArB-50**.[133] Both compounds exhibited bathochromic shifts and reduced photoluminescence intensity as solvent polarity increased, with **CZ-ArB-50** showing a stronger quenching effect. Phosphorescence spectra indicated the presence of triplet states in both compounds, with ΔE_{ST} values of 0.21 eV for **CZ-ArB-49** and 0.13 eV for **CZ-ArB-50**. The smaller ΔE_{ST} in **CZ-ArB-50**, due to the stronger electron-donating ability of phenoxazine, facilitated better triplet exciton harvesting, enhancing its TADF performance. OLEDs using **CZ-ArB-49** emitted deep-blue light (CIE: 0.16, 0.12) and achieved a maximum EQE of 5.5%, while those based on **CZ-ArB-50** exhibited a significantly higher EQE of 22.3% (CIE: 0.21, 0.45), demonstrating its superior efficiency for high-performance OLED devices with tunable emission.

Shi *et al.* synthesized two A–D–A type compounds, **CZ-ArB-51** and **CZ-ArB-52**, by incorporating $BMes_2$ or 4-$BMes_2$-phenyleneacetyl groups at the 2,7-positions of carbazole (Fig. 26), and explored the effects of introducing an aromatic phenylacetylene bridge on their geometric and electronic properties.[134] The study focused on the spectral modifications and photophysical behavior of these compounds, particularly their photoluminescence quantum yield (Φ_F) and fluorescence lifetime (τ_F). This structural modification resulted in a significantly

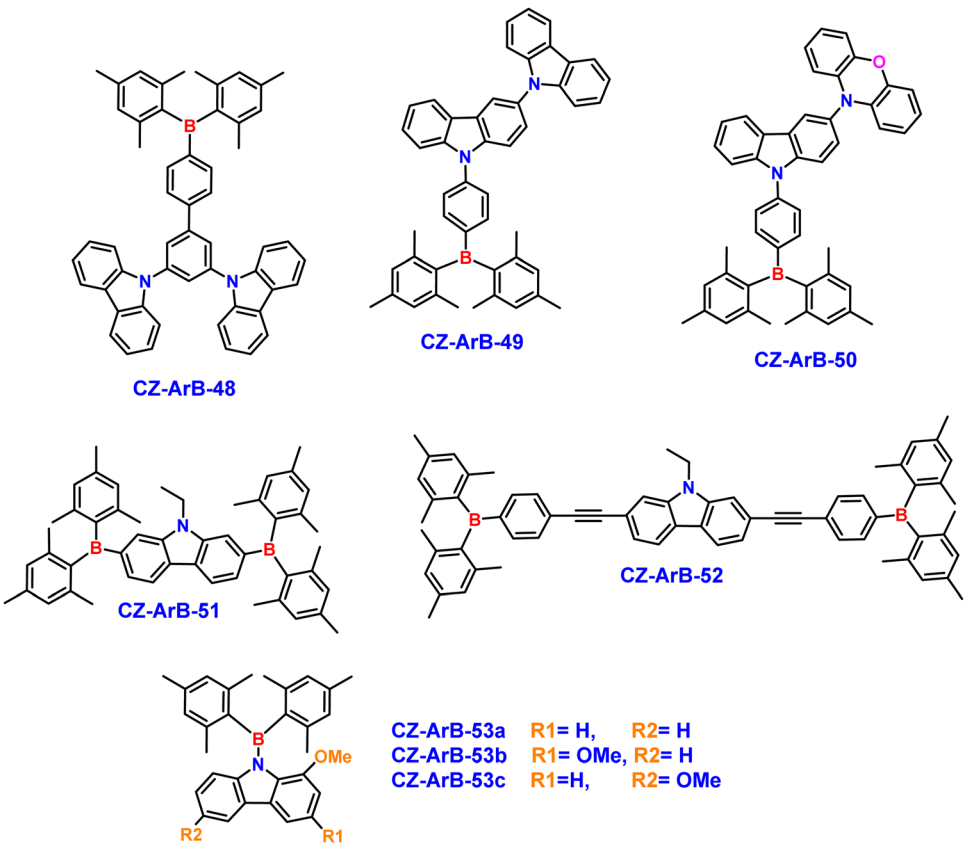

Fig. 26 Structure of compounds **CZ-ArB-48–53c**.

higher quantum yield (Φ_F = 0.95) and a shorter fluorescence lifetime (τ_F = 0.6 ns), likely due to a faster radiative decay rate of 1.6×10^9 s^{-1}, compared to the slower rate of 1.3×10^8 s^{-1} in **CZ-ArB-51**. Despite these differences, both compounds exhibited similar non-radiative decay rates. At 77 K in toluene, both compounds showed phosphorescence, with **CZ-ArB-52** demonstrating a remarkably long phosphorescence lifetime of up to 3 seconds. While the absorption spectra of both compounds were largely insensitive to solvent polarity, the PL spectra displayed a redshift and loss of structure, indicating increased polarity in the excited state relative to the ground state. In solid-state environments, such as PMMA films and powder forms, both compounds exhibited red-shifted PL with broader emission features and significantly longer lifetimes compared to their behavior in hexane.

In 2022, Ye *et al.* explored the photophysical mechanisms of boron dimesityl-based TADF emitters, specifically targeting a series of methoxy-carbazole (Cz)-substituted compounds (**CZ-ArB-53a–c**) (Fig. 26).[135] Through computational techniques such as DFT, TD-DFT, and DFT/multireference configuration interaction (DFT/MRCI), they analyzed the excited-state behavior of these molecules in cyclohexane. The study revealed that the electronic transitions responsible for absorption and emission between the ground state (S_0) and first singlet excited state (S_1) were primarily charge-transfer in nature. The HOMO was predominantly localized on the carbazole unit, while the LUMO resided on the bismesityl boron moiety. This clear spatial separation contributed to a very small $\Delta E_{ST} < 0.13$ eV, a critical factor in facilitating rISC. At ambient conditions, the compounds demonstrated efficient rISC, enabling delayed fluorescence due to balanced rates of fluorescence and ISC. However, the rISC process showed a strong dependency on temperature. At lower temperatures (77 K), the rate of rISC decreased significantly, leading to a suppression of delayed fluorescence and a reduced contribution from the triplet states to the overall emission. Phosphorescence remained negligible under all conditions, further emphasizing the dominance of TADF at higher temperatures.

In 2023, Cao *et al.* developed two innovative photo-activated room-temperature phosphorescent (RTP) materials, **CZ-ArB-54** and **CZ-ArB-55**, featuring a methylene carbazole functional unit positioned *ortho* to the aminoborane group (Fig. 27).[136] These compounds were embedded in PMMA films, resulting in enhanced RTP properties. Under 365 nm UV light in air, **CZ-ArB-55** exhibited a phosphorescence lifetime of 0.18 seconds with a quantum yield of 6.83%. Remarkably, when tested under a nitrogen atmosphere, the lifetime extended to 0.42 seconds, and the quantum yield increased to 17.34%, showcasing the significant role of environmental conditions on RTP performance. The versatility of the boron–nitrogen (BN) D–π–A system was highlighted by its ability to support RTP across a variety of substitutions. The attachment of electron-donating or electron-withdrawing groups at the *ortho* or *meta* positions of the boron atom produced a series of materials with tunable multi-color emissions, high quantum efficiencies, and extended phosphorescence lifetimes. These attributes make these materials ideal candidates for applications such as secure data storage, anti-counterfeiting measures, and durable water-resistant coatings (Fig. 28). To further enhance the performance, a pseudo-halogen functional group (CN) was introduced at the *ortho* position of the boron atom. This structural modification significantly increased both the phosphorescence lifetime and the quantum yield, with BN-*o*-CN@PMMA films achieving a lifetime of 1.40 seconds and a quantum yield of 7.94%. Detailed experimental and theoretical analyses revealed that the incorporation of such groups enhanced intramolecular charge transfer (ICT) and facilitated the stabilization of triplet excitons, which are essential for efficient RTP. This

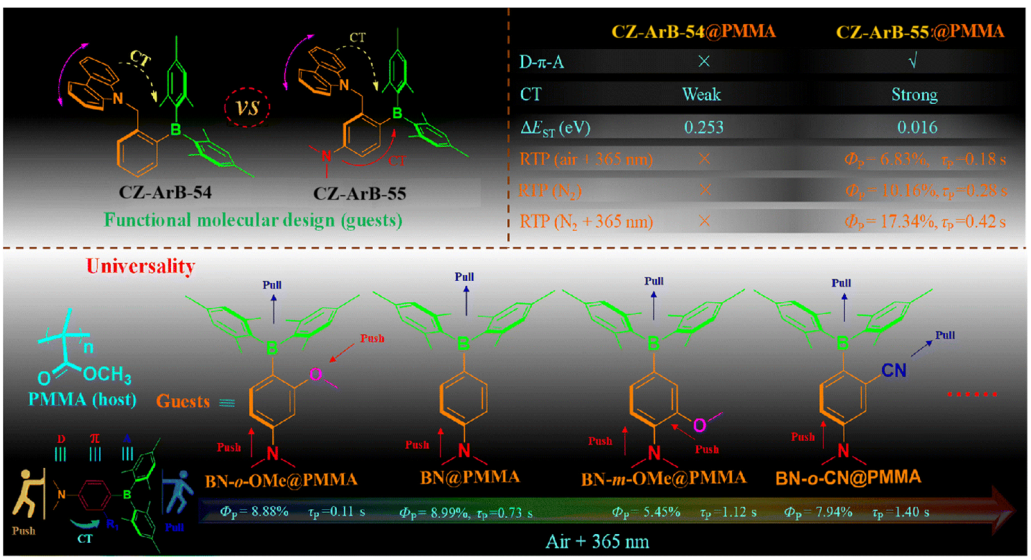

Fig. 27 Chemical structure of compounds **CZ-ArB-54** and **CZ-ArB-55**, BN, BN-*o*-OMe, BN-*m*-OMe, and BN-*o*-CN. Reproduced with permission from ref. 136. Copyright 2023 Royal Society of Chemistry.

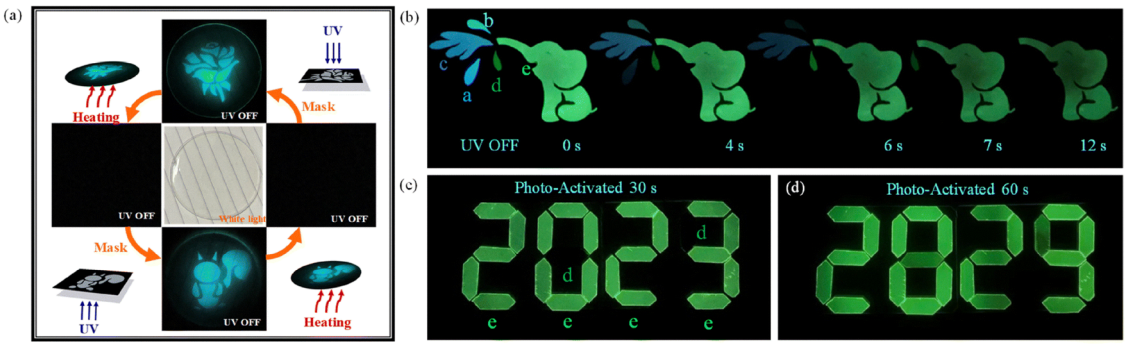

Fig. 28 (a) Application of programmable optical information writing/erasing based on **CZ-ArB-55**@PMMA. (b) Elephant spray pattern made of films a to e. (c) An application of information encryption: upon exposure to 365 nm UV light for 30 seconds, film E was activated to reveal the hidden message "2023". (d) Upon extension of the irradiation time to 60 s, the film d was also activated to display the information of "2829". Film a: BN-*o*-OMe@PMMA; film b: BN-*o*-Met-Cz@PMMA; film c: BN@PMMA; film d: BN-*m*-OMe@PMMA; film e: BN-*o*-CN@PMMA. Reproduced with permission from ref. 136. Copyright 2023 Royal Society of Chemistry.

study underscores a transformative approach to designing and optimizing organic RTP materials by leveraging the interplay between molecular structure and photophysical properties.

4. Conclusion and future outlook

This review provides a comprehensive synthesis of advancements in carbazole–triarylboranes compounds, consolidating progress made between 2005 and 2025. These compounds have firmly established themselves as pivotal components in the development of optoelectronic materials, particularly for applications requiring high solid-state emission efficiencies, tunable photophysical properties, and robust performance. The unique combination of carbazole's electron-donating ability and strong electron-accepting nature of TAB has allowed researchers to design molecular systems that excel across diverse platforms, including AIE, TADF, and OLEDs. A remarkable feature of carbazole–TAB systems is their ability to overcome the challenge of ACQ, a common limitation in luminescent materials. Through careful molecular design, researchers have developed systems that enhance emission upon aggregation, leveraging AIE mechanisms to create materials with robust solid-state performance. This has been particularly beneficial for OLED technology, where efficient solid-state emission and solution processability are critical for device fabrication. Moreover, the strategic tuning of singlet–triplet energy gaps in carbazole-boron systems has enabled efficient RISC, a process integral to TADF. By achieving near-unity internal quantum efficiencies, these systems have revolutionized OLEDs, delivering devices with exceptional color purity, high brightness, and energy efficiency. In addition to their solid-state applications, carbazole–TAB systems have found utility in bioimaging and chemical sensing and environmental sensitivity. Their ability to detect changes in the local environment has also been harnessed for chemical sensing, allowing for the development of systems with remarkable selectivity and sensitivity. These contributions underline the versatility of carbazole–TAB systems, demonstrating their potential across multiple domains.

Despite significant progress, challenges persist that hinder the full potential of carbazole–TAB systems. A key issue is the air and moisture sensitivity of certain TAB derivatives, which can undermine their stability and practical use. Addressing this challenge will necessitate innovative molecular design strategies, such as incorporating steric protection around boron centers or creating boron–oxygen and boron–nitrogen frameworks to improve their resilience under ambient conditions. Another challenge is achieving a balance between outstanding performance and long-term operational stability in carbazole–TAB systems. While many compounds deliver impressive initial results, their durability and stability over prolonged use or continuous device operation still require further optimization. Scalability remains another critical hurdle. Current synthetic methods for carbazole–TAB compounds are often complex, costly, and environmentally harmful, involving multiple reaction steps. To enable broader industrial adoption, more efficient, cost-effective, and sustainable production techniques need to be developed. Looking ahead, the future of carbazole–TAB systems is filled with exciting possibilities. One promising direction is exploring advanced applications, particularly in circularly polarized luminescence (CPL), room-temperature phosphorescence (RTP), and multifunctional capabilities such as anticounterfeiting. CPL-active carbazole–TAB systems, with their ability to generate high dissymmetry factors, show great promise for applications in three-dimensional displays, quantum computing, and secure information encryption. In the biomedical sector, these compounds are becoming increasingly popular as bioimaging probes due to their high photostability, excellent fluorescence quantum yields, and tunable emission properties, which make them ideal for cellular and *in vivo* imaging. Enhancing water solubility and biocompatibility through functional group modifications is also expanding their potential for biological applications. Furthermore, carbazole–TAB systems are gaining attention as selective chemical sensors, opening up new avenues for environmental

monitoring, disease detection, and personalized medicine. In photodynamic therapy (PDT), carbazole–TAB compounds with extended π-conjugation can act as efficient photosensitizers, generating reactive oxygen species (ROS) upon light exposure to selectively target cancer cells, offering a non-invasive approach to cancer treatment. Advances in two-photon absorption (TPA) characteristics are also enhancing their potential for deep-tissue PDT, improving treatment precision and minimizing side effects. Another rapidly growing area is anticounterfeiting, where the unique photophysical properties of carbazole–TAB systems, such as tunable emission and CPL activity, can be leveraged to develop advanced security materials. By embedding these compounds into authentication labels or anti-counterfeit devices, highly reliable and hard-to-replicate security features can be created, benefiting industries such as pharmaceuticals, luxury goods, and financial documents. The integration of carbazole–TAB systems into emerging technologies like flexible electronics and wearable devices presents another exciting Frontier. With their outstanding optical and electronic properties, these compounds have the potential to revolutionize the design of next-generation wearable optoelectronic devices, offering functionalities such as flexible OLEDs, light-emitting sensors, and smart textiles. Additionally, the combination of carbazole–TAB systems with other functional materials, such as polycyclic aromatic hydrocarbons or metal–organic frameworks, could lead to the development of new materials with enhanced performance and unique capabilities. Sustainability will be crucial in shaping the future of carbazole–TAB systems. As demand for environmentally friendly materials rises, efforts will focus on developing greener synthetic routes that reduce energy consumption, minimize waste, and avoid toxic solvents. Achieving more sustainable production methods will be essential for the commercial scalability and widespread adoption of these materials. Finally, computational and theoretical tools will play a vital role in optimizing carbazole–TAB systems. Advanced quantum chemical modelling and machine learning algorithms will accelerate the discovery of new compounds, reduce reliance on trial-and-error experimentation, and help rapidly develop high-performance materials.

In conclusion, the evolution of carbazole–TAB systems over the past two decades has underscored their transformative potential in a wide range of applications. These compounds have bridged fundamental scientific advancements with practical technological developments, demonstrating unparalleled versatility and innovation. By addressing the current challenges and seizing emerging opportunities, researchers are poised to unlock the next generation of high-performance luminescent materials. The synergy between carbazole and TAB continues to drive new Frontiers in materials science, with the promise of revolutionizing fields ranging from optoelectronics to biomedicine and anticounterfeiting. With ongoing advancements in design, synthesis, and applications, carbazole–TAB compounds are well-positioned to play a central role in the future of functional materials, paving the way for groundbreaking developments in solid-state emission, energy-efficient technologies, and beyond.

Abbreviations

AIE	Aggregation-induced emission
AIEE	Aggregation-induced emission enhancement
ICT	Intramolecular charge transfer
TADF	Thermally activated delayed fluorescence
TICT	Twisted intramolecular charge transfer
MFC	Mechanofluorochromism
OLED	Organic light-emitting diodes
OPVs	Organic photovoltaics
ACQ	Aggregation-caused quenching
SEM	Scanning electron microscope
THF	Tetrahydrofuran
PXRD	Powder X-ray diffraction
DFT	Density functional theory
NMR	Nuclear magnetic resonance
rISC	Reverse inter system crossing
PE	Power efficiency
EQE	External quantum efficiency
LOD	Limit of detection
TD-DFT	Time-dependent density-functional theory

Author contributions

A. A – conceptualization, data curation, formal analysis, investigation, visualization, writing – original draft. C. A. S. P – supervision, resources, validation, writing – review & editing.

Data availability

No original research findings, software, or code were included, and no new data were generated or analyzed as part of this review.

Conflicts of interest

The authors declare no competing financial interest.

Acknowledgements

CAS P acknowledges the research grant SERB/EEQ/2021/000180 and. A. A thanks the National Institute of Technology, Calicut, for GATE-JRF fellowship.

References

1 J. Bauri, R. B. Choudhary and G. Mandal, Recent advances in efficient emissive materials-based OLED applications: a review, *J. Mater. Sci.*, 2021, **56**, 18837.
2 S. J. Zou, Y. Shen, F. M. Xie, J. D. Chen, Y. Q. Li and J. X. Tang, Recent advances in organic light-emitting diodes: toward smart lighting and displays, *Mater. Chem. Front.*, 2020, **4**, 788.
3 A. Salehi, X. Fu, D. H. Shin and F. So, Recent advances in OLED optical design, *Adv. Funct. Mater.*, 2019, **29**, 1808803.

4 J. Y. Woo, M. H. Park, S. H. Jeong, Y. H. Kim, B. Kim, T. W. Lee and T. H. Han, Advances in solution-processed OLEDs and their prospects for use in displays, *Adv. Mater.*, 2023, **35**, 2207454.
5 Y. Xu, P. Xu, D. Hu and Y. Ma, Recent progress in hot exciton materials for organic light-emitting diodes, *Chem. Soc. Rev.*, 2021, **50**, 1030.
6 Y. Jiang, Y. Y. Liu, X. Liu, H. Lin, K. Gao, W. Y. Lai and W. Huang, Organic solid-state lasers: a materials view and future development, *Chem. Soc. Rev.*, 2020, **49**, 5885.
7 H. H. Fang, J. Yang, J. Feng, T. Yamao, S. Hotta and H. B. Sun, Functional organic single crystals for solid-state laser applications, *Laser Photonics Rev.*, 2014, **8**, 687.
8 G. Q. Wei, X. D. Wang and L. S. Liao, Recent Advances in 1D Organic Solid-State Lasers, *Adv. Funct. Mater.*, 2019, **29**, 1902981.
9 J. J. Wu, X. D. Wang and L. S. Liao, Near-infrared solid-state lasers based on small organic molecules, *ACS Photonics*, 2019, **6**, 2590.
10 I. M. Khan, S. Niazi, M. K. I. Khan, I. Pasha, A. Mohsin, J. Haider, M. W. Iqbal, A. Rehman, L. Yue and Z. Wang, Recent advances and perspectives of aggregation-induced emission as an emerging platform for detection and bioimaging, *Trends Anal. Chem.*, 2019, **119**, 115637.
11 H. Lu, Y. Zheng, X. Zhao, L. Wang, S. Ma, X. Han, B. Xu, W. Tian and H. Gao, Highly efficient far Red/Near-infrared solid fluorophores: aggregation-induced emission, intramolecular charge transfer, twisted molecular conformation, and bioimaging applications, *Angew. Chem., Int. Ed.*, 2016, **55**, 155.
12 K. Li, T. B. Ren, S. Huan, L. Yuan and X. B. Zhang, Progress and perspective of solid-state organic fluorophores for biomedical applications, *J. Am. Chem. Soc.*, 2021, **143**, 21143.
13 H. Cao, Y. Gao, B. Wu, J. Zhang, L. Wang, P. Wei, L. Liu, H. Zou, H. Zhou, Z. Zheng and B. Z. Tang, Tuning Molecular Packing by Twisting Structure to Facilely Construct Highly Efficient Solid-State Fluorophores for Two-Photon Bioimaging and Photodynamic Therapy, *Adv. Funct. Mater.*, 2024, **34**, 2315692.
14 Y. Zhang, J. Zhang, J. Shen, J. Sun, K. Wang, Z. Xie, H. Gao and B. Zou, Solid-State TICT-Emissive Cruciform: Aggregation-Enhanced Emission, Deep-Red to Near-Infrared Piezochromism and Imaging In Vivo, *Adv. Opt. Mater.*, 2018, **6**, 1800956.
15 L. Wang, L. Yang and D. Cao, Application of aggregation-induced emission (AIE) systems in sensing and bioimaging, *Curr. Org. Chem.*, 2014, **18**, 1028.
16 P. Gayathri, M. Pannipara, A. G. Al-Sehemi and S. P. Anthony, Recent advances in excited state intramolecular proton transfer mechanism-based solid state fluorescent materials and stimuli-responsive fluorescence switching, *CrystEngComm*, 2021, **23**, 3771.
17 S. Jaiswal, S. Das, S. Kundu, I. Rawal, P. Anand and A. Patra, Progress and perspectives: fluorescent to long-lived emissive multifunctional probes for intracellular sensing and imaging, *J. Mater. Chem. C*, 2022, **10**, 6141.
18 M. Gao and B. Z. Tang, Fluorescent sensors based on aggregation-induced emission: recent advances and perspectives, *ACS Sens.*, 2017, **2**, 1382.
19 J. Luo, Z. Xie, J. W. Lam, L. Cheng, H. Chen, C. Qiu, H. S. Kwok, X. Zhan, Y. Liu, D. Zhu and B. Z. Tang, Aggregation-induced emission of 1-methyl-1,2,3,4,5-pentaphenylsilole, *Chem. Commun.*, 2001, 1740.
20 A. Zampetti, A. Minotto and F. Cacialli, Near-Infrared (NIR) Organic Light-Emitting Diodes (OLEDs): Challenges and Opportunities, *Adv. Funct. Mater.*, 2019, **29**, 1807623.
21 C. Li, R. Duan, B. Liang, G. Han, S. Wang, K. Ye, Y. Liu, Y. Yi and Y. Wang, Deep-Red to Near-Infrared Thermally Activated Delayed Fluorescence in Organic Solid Films and Electroluminescent Devices, *Angew. Chem., Int. Ed.*, 2017, **129**, 11683.
22 J. X. Chen, W. W. Tao, W. C. Chen, Y. F. Xiao, K. Wang, C. Cao, J. Yu, S. Li, F. X. Geng, C. Adachi and C. S. Lee, Red/Near-Infrared Thermally Activated Delayed Fluorescence OLEDs with Near 100% Internal Quantum Efficiency, *Angew. Chem., Int. Ed.*, 2019, **131**, 14802.
23 Y. Li, J. Yao, C. Wang, X. Zhou, Y. Xu, M. Hanif, X. Qiu, D. Hu, D. Ma and Y. Ma, Highly efficient deep-red/near-infrared DA chromophores based on naphthothiadiazole for OLEDs applications, *Dyes Pigm.*, 2020, **173**, 107960.
24 Kenry, Y. Duan and B. Liu, Recent advances of optical imaging in the second near-infrared window, *Adv. Mater.*, 2018, **30**, 1802394.
25 A. Minotto, P. A. Haigh, G. Łukasiewicz, E. Lunedei, D. T. Gryko, I. Darwazeh and F. Cacialli, Visible light communication with efficient far-red/near-infrared polymer light-emitting diodes, *Light: Sci. Appl.*, 2020, **9**, 170.
26 Y. Ning, M. Zhu and J. L. Zhang, Near-infrared (NIR) lanthanide molecular probes for bioimaging and biosensing, *Coord. Chem. Rev.*, 2019, **399**, 213028.
27 L. Yuan, W. Lin, K. Zheng, L. He and W. Huang, Far-red to near infrared analyte-responsive fluorescent probes based on organic fluorophore platforms for fluorescence imaging, *Chem. Soc. Rev.*, 2013, **42**, 622.
28 M. Dai, Y. J. Yang, S. Sarkar and K. H. Ahn, Strategies to convert organic fluorophores into red/near-infrared emitting analogues and their utilization in bioimaging probes, *Chem. Soc. Rev.*, 2023, **52**, 6344.
29 Y. Chen, L. Xue, Q. Zhu, Y. Feng and M. Wu, Recent advances in second near-infrared region (NIR-II) fluorophores and biomedical applications, *Front. Chem.*, 2021, **9**, 750404.
30 X. K. Chen, D. Kim and J. L. Brédas, Thermally activated delayed fluorescence (TADF) path toward efficient electroluminescence in purely organic materials: molecular level insight, *Acc. Chem. Res.*, 2018, **51**, 2215.
31 Y. Liu, C. Li, Z. Ren, S. Yan and M. R. Bryce, All-organic thermally activated delayed fluorescence materials for organic light-emitting diodes, *Nat. Rev. Mater.*, 2018, **3**, 1.
32 T. Huang, W. Jiang and L. Duan, Recent progress in solution processable TADF materials for organic light-emitting diodes, *J. Mater. Chem. C*, 2018, **6**, 577.

33 J. M. Teng, Y. F. Wang and C. F. Chen, Recent progress of narrowband TADF emitters and their applications in OLEDs, *J. Mater. Chem. C*, 2020, **8**, 11340.
34 J. M. Dos Santos, D. Hall, B. Basumatary, M. Bryden, D. Chen, P. Choudhary, T. Comerford, E. Crovini, A. Danos, J. De and S. Diesing, The golden age of thermally activated delayed fluorescence materials: design and exploitation, *Chem. Rev.*, 2024, **124**, 13736.
35 P. Ledwon, Recent advances of donor-acceptor type carbazole-based molecules for light emitting applications, *Org. Electron.*, 2019, **75**, 105422.
36 A. Sharma, D. Saklani, K. J. Thomas, S. S. Swayamprabha and J. H. Jou, Synthesis and characterization of multi-substituted carbazole derivatives exhibiting aggregation-induced emission for OLED applications, *Org. Electron.*, 2020, **86**, 105864.
37 B. Wex and B. R. Kaafarani, Perspective on carbazole-based organic compounds as emitters and hosts in TADF applications, *J. Mater. Chem. C*, 2017, **5**, 8622.
38 H. Jiang, J. Sun and J. Zhang, A review on synthesis of carbazole-based chromophores as organic light-emitting materials, *Curr. Org. Chem.*, 2012, **16**, 2014.
39 J. Yin, Y. Ma, G. Li, M. Peng and W. Lin, A versatile small-molecule fluorescence scaffold: carbazole derivatives for bioimaging, *Coord. Chem. Rev.*, 2020, **412**, 213257.
40 S. Oner and M. R. Bryce, A review of fused-ring carbazole derivatives as emitter and/or host materials in organic light emitting diode (OLED) applications, *Mater. Chem. Front.*, 2023, **7**, 4304.
41 R. K. Konidena, K. J. Thomas and J. W. Park, Recent advances in the design of multi-substituted carbazoles for optoelectronics: synthesis and structure–property outlook, *ChemPhotoChem*, 2022, **6**, 202200059.
42 A. Afrin and P. C. A. Swamy, Symphony of light: AIE and MFC in carbazole-based cyanostilbenes, *J. Mater. Chem. C*, 2024, **12**, 1923.
43 B. Prusti and M. Chakravarty, Disparity in piezofluorochromism for twisted mono-carbazole-based AIEgens resulting from interchanging electron-rich substituents: effect of coplanarity on twisted π-conjugates, *Mater. Adv.*, 2021, **2**, 1752.
44 C. H. Chang, R. Griniene, Y. D. Su, C. C. Yeh, H. C. Kao, J. V. Grazulevicius, D. Volyniuk and S. Grigalevicius, Efficient red phosphorescent OLEDs employing carbazole-based materials as the emitting host, *Dyes Pigm.*, 2015, **122**, 257.
45 B. Ruan, X. Kang, B. Guo, D. D. Deng, J. J. Tian, K. He, X. Y. Wang, S. Pu and Z. Chen, Donor-donor-acceptor (DDA) luminogens containing a central carbazole core: aggregation-induced emission (AIE), full-color solid-state emission and diverse mechanofluorochromic characteristics, *J. Mol. Struct.*, 2024, **1309**, 138171.
46 M. Mamada, M. Hayakawa, J. Ochi and T. Hatakeyama, Organoboron-based multiple-resonance emitters: synthesis, structure–property correlations, and prospects, *Chem. Soc. Rev.*, 2024, **53**, 1624.
47 S. K. Mellerup and S. Wang, Boron-based stimuli responsive materials, *Chem. Soc. Rev.*, 2019, **48**, 3537.
48 Z. Huang, S. Wang, R. D. Dewhurst, N. V. Ignat'ev, M. Finze and H. Braunschweig, Boron: its role in energy-related processes and applications, *Angew. Chem., Int. Ed.*, 2020, **59**, 8800.
49 S. Mukherjee and P. Thilagar, Stimuli and shape responsive boron-containing luminescent organic materials, *J. Mater. Chem. C*, 2016, **4**, 2647.
50 R. K. Konidena and K. R. Naveen, Boron-Based Narrowband Multiresonance Delayed Fluorescent Emitters for Organic Light-Emitting Diodes, *Adv. Photonics Res.*, 2022, **3**, 2200201.
51 G. Turkoglu, M. E. Cinar and T. Ozturk, Triarylborane-based materials for OLED applications, *Molecules*, 2017, **22**, 1522.
52 J. Huo, H. Wang, S. Li, H. Shi, Y. Tang and B. Z. Tang, Design and Development of Highly Efficient Light-Emitting Layers in OLEDs with Dimesitylboranes: An Updated Review, *Chem. Rec.*, 2020, **20**, 556.
53 J. Shi, Z. Ran, F. Peng, M. Chen, L. Li, L. Ji and W. Huang, High-performance three-coordinated organoboron emitters for organic light-emitting diodes, *J. Mater. Chem. C*, 2022, **10**, 9165.
54 S. Shao and L. Wang, Through-space charge transfer polymers for solution-processed organic light-emitting diodes, *Aggregate*, 2020, **1**, 45.
55 C. D. Entwistle and T. B. Marder, Applications of three-coordinate organoboron compounds and polymers in optoelectronics, *Chem. Mater.*, 2004, **16**, 4574.
56 J. Kim, T. Lee, J. Y. Ryu, Y. H. Lee, J. Lee, J. Jung and M. H. Lee, Highly emissive *ortho*-donor–acceptor triarylboranes: impact of boryl acceptors on luminescence properties, *Organometallics*, 2020, **39**, 2235.
57 H. Lee, S. Jana, J. Kim, S. U. Lee and M. H. Lee, Donor–Acceptor-Appended Triarylboron Lewis Acids: Ratiometric or Time-Resolved Turn-On Fluorescence Response toward Fluoride Binding, *Inorg. Chem.*, 2020, **59**, 1414.
58 N. Aota, R. Nakagawa, L. E. de Sousa, N. Tohnai, S. Minakata, P. de Silva and Y. Takeda, Anion-Responsive Colorimetric and Fluorometric Red-Shift in Triarylborane Derivatives: Dual Role of Phenazaborine as Lewis Acid and Electron Donor, *Angew. Chem., Int. Ed.*, 2024, **63**, 202405158.
59 C. Wang, Y. Yuan, S. Y. Li, Z. B. Sun, Z. Q. Jiang and C. H. Zhao, A highly twisted triarylborane-based biphenyl as an efficient host for blue and green phosphorescent OLEDs, *J. Mater. Chem. C*, 2016, **4**, 7607.
60 M. Liu, H. Hao, G. Liao, C. Li, K. Liu, N. Wang, Q. Niu and X. Yin, Boron-Containing Molecules with Fluorescence-Phosphorescence Dual-Emission for Mechanochromism and Single Molecular White Light-Emitting Diodes, *Adv. Opt. Mater.*, 2023, **11**, 2202918.
61 J. Shi, Z. Ran, F. Peng, M. Chen, L. Li, L. Ji and W. Huang, High-performance three-coordinated organoboron emitters for organic light-emitting diodes, *J. Mater. Chem. C*, 2022, **10**, 9165–9191.

62 X. Jia, J. Nitsch, L. Ji, Z. Wu, A. Friedrich, F. Kerner, M. Moos, C. Lambert and T. B. Marder, Triarylborane-Based Helical Donor–Acceptor Compounds: Synthesis, Photophysical, and Electronic Properties, *Chem. – Eur. J.*, 2019, **25**, 10845.

63 A. Lorente, P. Pingel, H. Krüger and S. Janietz, High triplet energy electron transport side-chain polystyrenes containing dimesitylboron and tetraphenylsilane for solution processed OLEDs, *J. Mater. Chem. C*, 2017, **5**, 10660.

64 J. L. Ma, H. Liu, S. Y. Li, Z. Y. Li, H. Y. Zhang, Y. Wang and C. H. Zhao, Metal-free room-temperature phosphorescence from amorphous triarylborane-based biphenyl, *Organometallics*, 2020, **39**, 4153.

65 Z. Wu, J. Nitsch, J. Schuster, A. Friedrich, K. Edkins, M. Loebnitz, F. Dinkelbach, V. Stepanenko, F. Würthner, C. M. Marian and L. Ji, Persistent room temperature phosphorescence from triarylboranes: a combined experimental and theoretical study, *Angew. Chem., Int. Ed.*, 2020, **59**, 17137.

66 R. Arumugam, A. T. M. Munthasir, R. Kannan, D. Banerjee, P. Sudhakar, V. R. Soma, P. Thilagar and V. Chandrasekhar, Regioisomers containing triarylboron-based motifs as multi-functional photoluminescent materials: from dual-mode delayed emission to pH-switchable room-temperature phosphorescence, *Chem. Sci.*, 2024, **15**, 18364–18378.

67 Y. Xie, S. Dai, Y. Wang, X. Wang, Y. Sun, Z. Ju, R. Fang, B. Zhang, J. Wu, X. Zhang and X. Pan, Structural and mechanistic studies of excitation-and temperature-tunable multicolor luminescence of triarylborane, *CrystEngComm*, 2023, **25**, 2204.

68 H. E. Hackney and D. F. Perepichka, Recent advances in room temperature phosphorescence of crystalline boron containing organic compounds: Nanoscience: Special Issue Dedicated to Professor Paul S. Weiss, *Aggregate*, 2022, **3**, 123.

69 P. C. A. Swamy and P. Thilagar, Triarylborane-appended new triad and tetrad: chromogenic and fluorogenic anion recognition, *Inorg. Chem.*, 2014, **53**, 2776.

70 P. C. A. Swamy, S. Mukherjee and P. Thilagar, Dual emissive borane–BODIPY dyads: molecular conformation control over electronic properties and fluorescence response towards fluoride ions, *Chem. Commun.*, 2013, **49**, 993.

71 R. Misra, T. Jadhav, B. Dhokale and S. M. Mobin, Colorimetric and fluorimetric detection of fluoride and cyanide ions using tri and tetra coordinated boron containing chromophores, *Dalton Trans.*, 2015, **44**, 16052.

72 K. C. Song, H. Kim, K. M. Lee, Y. S. Lee, Y. Do and M. H. Lee, Ratiometric fluorescence sensing of fluoride ions by triarylborane–phenanthroimidazole conjugates, *Sens. Actuators, B*, 2013, **176**, 850.

73 P. C. A. Swamy and P. Thilagar, Multiple emissive triarylborane-A_2H_2 and triarylborane-Zn-A_2H_2 porphyrin conjugates, *Dalton Trans.*, 2016, **45**, 4688–4696.

74 A. Afrin and P. C. A. Swamy, Tailoring Emission Color shifts in Mechanofluorochromic Active AIE Systems of Carbazole-Based D–π–A conjugates: Impact of π Spacer Unit Variants, *J. Org. Chem.*, 2024, **89**, 7946.

75 A. Afrin and P. C. A. Swamy, Aggregation Induced Emission and Reversible Mechanofluorochromism Active Carbazole-Anthracene Conjugated Cyanostilbenes with Different Terminal Substitutions, *New J. Chem.*, 2023, **47**, 18919.

76 A. Afrin and P. C. A. Swamy, π-Spacer Engineering: Driving Near-Infrared Aggregation Induced-Emission and Mechanofluorochromism in Carbazole-Biscyanostilbenes, *Chem. – Eur. J.*, 2025, **31**, 202403644.

77 P. C. A. Swamy and A. V. Raveendran, Triarylborane–Triphenylamine Based Donor–Acceptor Fluorophores as pH and Fluoride Sensors, *ChemistrySelect*, 2024, **9**, 202305115.

78 A. V. Raveendran and P. C. A. Swamy, Fine-tuning the Acceptor–Donor Ability of Star Shaped Triarylborane–Triphenylamine Conjugates: Synthesis, Characterization, and Anion Binding Studies, *New J. Chem.*, 2022, **46**, 20299.

79 P. C. A. Swamy, A. V. Raveendran, N. Sivakrishna and P. N. Rajendra, Triarylborane-triphenylamine based luminophore for the mitochondria-targeted live cell imaging and colorimetric detection of aqueous fluoride, *Dalton Trans.*, 2022, **51**, 15339.

80 N. Altinolcek, A. Battal, C. N. Vardalli, M. Tavasli, A. Y. Holly, W. J. Peveler and P. J. Skabara, Carbazole-based D–π–A molecules: Determining the photophysical properties and comparing ICT effects of π-spacer and acceptor groups, *J. Mol. Struct.*, 2021, **1239**, 130494.

81 J. Tagare, R. Boddula, R. A. K. Yadav, D. K. Dubey, J. H. Jou, S. Patel and S. Vaidyanathan, Novel imidazole-alkyl spacer-carbazole based fluorophores for deep-blue organic light emitting diodes: experimental and theoretical investigation, *Dyes Pigm.*, 2021, **185**, 108853.

82 P. Wen, Z. Gao, R. Zhang, A. Li, F. Zhang, J. Li, J. Xie, Y. Wu, M. Wu and K. Guo, A–π–D–π–A carbazole derivatives with remarkable solvatochromism and mechanoresponsive luminescence turn-on, *J. Mater. Chem. C*, 2017, **5**, 6136.

83 H. Wang, X. Shen, J. Ge, Y. Deng, F. Ding, Z. Wang, W. Zhu, L. Hu, J. He and X. Gu, Rational design of AIE-based carbazole derivatives for lipid droplet-specific imaging in living cells, *Chem. Pap.*, 2023, **77**, 563.

84 H. S. Kumbhar, S. S. Deshpande and G. S. Shankarling, Aggregation induced emission (AIE) active carbazole styryl fluorescent molecular rotor as viscosity sensor, *ChemistrySelect*, 2016, **1**, 2058.

85 C. Liu, H. Luo, G. Shi, J. Yang, Z. Chi and Y. Ma, Luminescent network film deposited electrochemically from a carbazole functionalized AIE molecule and its application for OLEDs, *J. Mater. Chem. C*, 2015, **3**, 3752–3759.

86 T. H. Ha, J. K. Bin and C. W. Lee, Phenylpyridine and carbazole based host materials for highly efficient blue TADF OLEDs, *Org. Electron.*, 2022, **102**, 106450.

87 S. J. Lee, J. S. Park, K. J. Yoon, Y. I. Kim, S. H. Jin, S. K. Kang, Y. S. Gal, S. Kang, J. Y. Lee, J. W. Kang and S. H. Lee, High-efficiency deep-blue light-emitting diodes based on phenylquinoline/carbazole-based compounds, *Adv. Funct. Mater.*, 2008, **18**, 3922.

88 G. Sathiyan, E. K. T. Sivakumar, R. Ganesamoorthy, R. Thangamuthu and P. Sakthivel, Review of carbazole based conjugated molecules for highly efficient organic solar cell application, *Tetrahedron Lett.*, 2016, **57**, 243.
89 K. Maslowska-Jarzyna, M. L. Korczak, J. A. Wagner and M. J. Chmielewski, Carbazole-based colorimetric anion sensors, *Molecules*, 2021, **26**, 3205.
90 K. R. Justin Thomas, J. T. Lin, Y. T. Tao and C. W. Ko, Light-emitting carbazole derivatives: potential electroluminescent materials, *J. Am. Chem. Soc.*, 2001, **123**, 9404.
91 C. Liu, L. Yin and Y. Li, Organoboron-embedded functional materials: recent developments in photovoltaic and luminescence properties, *J. Mater. Chem. C*, 2024, **12**, 11723.
92 F. Jäkle, Advances in the synthesis of organoborane polymers for optical, electronic, and sensory applications, *Chem. Rev.*, 2010, **110**, 3985.
93 C. R. Wade, A. E. Broomsgrove, S. Aldridge and F. P. Gabbai, Fluoride ion complexation and sensing using organoboron compounds, *Chem. Rev.*, 2010, **110**, 3958.
94 S. Mukherjee and P. Thilagar, Organoborane Donor–Acceptor Materials, *Main Group Strategies Funct. Hybrid Mater.*, 2017, 27.
95 X. Jia, J. Nitsch, L. Ji, Z. Wu, A. Friedrich, F. Kerner, M. Moos, C. Lambert and T. B. Marder, Triarylborane-Based Helical Donor–Acceptor Compounds: Synthesis, Photophysical, and Electronic Properties, *Chem. – Eur. J.*, 2019, **25**, 10845.
96 B. Meng, Y. Ren, J. Liu, F. Jäkle and L. Wang, p–π Conjugated Polymers Based on Stable Triarylborane with n-Type Behavior in Optoelectronic Devices, *Angew. Chem., Int. Ed.*, 2018, **130**, 2205.
97 A. Ben Saida, A. Chardon, A. Osi, N. Tumanov, J. Wouters, A. I. Adjieufack, B. Champagne and G. Berionni, Pushing the Lewis Acidity Boundaries of Boron Compounds with Non-Planar Triarylboranes Derived from Triptycenes, *Angew. Chem., Int. Ed.*, 2019, **131**, 17045.
98 M. Wang and C. H. Zhao, Chiral Triarylborane-Based Small Organic Molecules for Circularly Polarized Luminescence, *Chem. Rec.*, 2022, **22**, 202100199.
99 R. Stahl, C. Lambert, C. Kaiser, R. Wortmann and R. Jakober, Electrochemistry and Photophysics of Donor-Substituted Triarylboranes: Symmetry Breaking in Ground and Excited State, *Chem. – Eur. J.*, 2006, **12**, 2358.
100 U. Megerle, F. Selmaier, C. Lambert, E. Riedle and S. Lochbrunner, Symmetry-dependent solvation of donor-substituted triarylboranes, *Phys. Chem. Chem. Phys.*, 2008, **10**, 6245.
101 S. L. Lin, L. H. Chan, R. H. Lee, M. Y. Yen, W. J. Kuo, C. T. Chen and R. J. Jeng, Highly efficient carbazole-π-dimesitylborane bipolar fluorophores for nondoped blue organic light-emitting diodes, *Adv. Mater.*, 2008, **20**, 3947.
102 D. Reitzenstein and C. Lambert, Localized versus backbone fluorescence in *N-p*-(diarylboryl) phenyl-substituted 2,7-and 3,6-linked polycarbazoles, *Macromolecules*, 2009, **42**, 773.
103 Y. H. Chen, Y. Y. Lin, Y. C. Chen, J. T. Lin, R. H. Lee, W. J. Kuo and R. J. Jeng, Carbazole/fluorene copolymers with dimesitylboron pendants for blue light-emitting diodes, *Polymer*, 2011, **52**, 976.
104 M. S. Lin, L. C. Chi, H. W. Chang, Y. H. Huang, K. C. Tien, C. C. Chen, C. H. Chang, C. C. Wu, A. Chaskar, S. H. Chou and H. C. Ting, A diarylborane-substituted carbazole as a universal bipolar host material for highly efficient electrophosphorescence devices, *J. Mater. Chem. C*, 2012, **22**, 870.
105 H. P. Shi, J. X. Dai, L. Xu, L. W. Shi, L. Fang, S. M. Shuang and C. Dong, A boron-containing carbazole dimer: synthesis, photophysical properties and sensing properties, *Org. Biomol. Chem.*, 2012, **10**, 3852.
106 H. P. Shi, J. X. Dai, L. W. Shi, M. H. Wang, L. Fang, S. M. Shuang and C. Dong, Aggregation induced ratiometric fluorescence change for a novel boron-based carbazole derivative, *Chem. Commun.*, 2012, **48**, 8586.
107 S. Zhang, Z. Qu, P. Tao, B. Brooks, Y. Shao, X. Chen and C. Liu, Quantum chemical study of the ground and excited state electronic structures of carbazole oligomers with and without triarylborane substitutes, *J. Phys. Chem. C*, 2012, **116**, 12434.
108 T. Taniguchi, J. Wang, S. Irle and S. Yamaguchi, TICT fluorescence of *N*-borylated 2,5-diarylpyrroles: a gear like dual motion in the excited state, *Dalton Trans.*, 2013, **42**, 620.
109 H. P. Shi, J. X. Dai, X. H. Wu, L. W. Shi, J. D. Yuan, L. Fang, Y. Q. Miao, X. G. Du, H. Wang and C. Dong, A novel dimesitylboron-substituted indolo[3,2-*b*]carbazole derivative: synthesis, electrochemical, photoluminescent and electroluminescent properties, *Org. Electron.*, 2013, **14**, 868.
110 H. Shi, J. Yang, X. Dong, L. Fang, C. Dong and M. M. Choi, A novel asymmetric indolo[3,2-*b*]carbazole derivative containing benzothiazole and dimesitylboron units: synthesis, photophysical and sensing properties, *Synth. Met.*, 2013, **179**, 42.
111 H. Shi, W. Zhang, X. Dong, X. Wu, Y. Wu, L. Fang, Y. Miao and H. Wang, A novel carbazole derivative containing dimesitylboron units: synthesis, photophysical, aggregation induced emission and electroluminescent properties, *Dyes Pigm.*, 2014, **104**, 34.
112 H. Shi, D. Xin, X. Dong, J. X. Dai, X. Wu, Y. Miao, L. Fang, H. Wang and M. M. Choi, A star-shaped bipolar host material based on carbazole and dimesitylboron moieties for fabrication of highly efficient red, green and blue electrophosphorescent devices, *J. Mater. Chem. C*, 2014, **2**, 2160.
113 H. G. Jang, B. S. Kim, J. Y. Lee and S. H. Hwang, Synthesis of dimesitylborane-substituted phenylcarbazoles as bipolar host materials and the variation of the green PHOLED performance with the substituent position of the boron atom, *Dalton Trans.*, 2014, **43**, 7712.
114 A. Ito, K. Kawanishi, E. Sakuda and N. Kitamura, Synthetic Control of Spectroscopic and Photophysical Properties of Triarylborane Derivatives Having Peripheral Electron-Donating Groups, *Chem. – Eur. J.*, 2014, **20**, 3940.

115 H. Shi, J. Yuan, X. Wu, X. Dong, L. Fang, Y. Miao, H. Wang and F. Cheng, Two novel indolo[3,2-*b*]carbazole derivatives containing dimesitylboron moieties: synthesis, photoluminescent and electroluminescent properties, *New J. Chem.*, 2014, **38**, 2368.

116 H. Shi, J. Yang, X. Dong, X. Wu, P. Zhou, F. Cheng and M. M. Choi, A novel tetraphenylethene–carbazole type compound containing the dimesitylboron moiety: aggregation-induced emission enhancement and electroluminescence properties, *RSC Adv.*, 2014, **4**, 19418.

117 H. Shi, Z. Gong, D. Xin, J. Roose, H. Peng, S. Chen, J. W. Lam and B. Z. Tang, Synthesis, aggregation-induced emission and electroluminescence properties of a novel compound containing tetraphenylethene, carbazole and dimesitylboron moieties, *J. Mater. Chem. C*, 2015, **3**, 9095.

118 H. Shi, D. Xin, X. Gu, P. Zhang, H. Peng, S. Chen, G. Lin, Z. Zhao and B. Z. Tang, The synthesis of novel AIE emitters with the triphenylethene-carbazole skeleton and *para*-/*meta*-substituted arylboron groups and their application in efficient non-doped OLEDs, *J. Mater. Chem. C*, 2016, **4**, 1228.

119 H. Shi, M. Li, D. Xin, L. Fang, J. Roose, H. Peng, S. Chen and B. Z. Tang, Two novel phenylethene-carbazole derivatives containing dimesitylboron groups: aggregation-induced emission and electroluminescence properties, *Dyes Pigm.*, 2016, **128**, 304.

120 X. Dong, M. Li, H. Shi, F. Cheng, J. Roose and B. Z. Tang, Synthesis, aggregation-induced emission, and electroluminescence of a new compound based on tetraphenylethene, carbazole, and dimesitylboron moieties, *Tetrahedron*, 2016, **72**, 2213.

121 H. Shi, D. Xin, S. D. Bai, L. Fang, X. E. Duan, J. Roose, H. Peng, S. Chen and B. Z. Tang, The synthesis, crystal structures, aggregation-induced emission and electroluminescence properties of two novel green-yellow emitters based on carbazole-substituted diphenylethene and dimesitylboron, *Org. Electron.*, 2016, **33**, 78.

122 H. Shi, X. Zhang, C. Gui, S. Wang, L. Fang, Z. Zhao, S. Chen and B. Z. Tang, Synthesis, aggregation-induced emission and electroluminescence properties of three new phenylethylene derivatives comprising carbazole and (dimesitylboranyl) phenyl groups, *J. Mater. Chem. C*, 2017, **5**, 11741.

123 K. Suzuki, S. Kubo, K. Shizu, T. Fukushima, A. Wakamiya, Y. Murata, C. Adachi and H. Kaji, Triarylboron-Based Fluorescent Organic Light-Emitting Diodes with External Quantum Efficiencies Exceeding 20%, *Angew. Chem., Int. Ed.*, 2015, **54**, 15231–15235.

124 Y. H. Lee, S. Park, J. Oh, J. W. Shin, J. Jung, S. Yoo and M. H. Lee, Rigidity-induced delayed fluorescence by *ortho* donor-appended triarylboron compounds: record-high efficiency in pure blue fluorescent organic light-emitting diodes, *ACS Appl. Mater. Interfaces*, 2017, **9**, 24035.

125 Y. H. Lee, S. Park, J. Oh, S. J. Woo, A. Kumar, J. J. Kim, J. Jung, S. Yoo and M. H. Lee, High-Efficiency Sky Blue to Ultradeep Blue Thermally Activated Delayed Fluorescent Diodes Based on Ortho-Carbazole-Appended Triarylboron Emitters: Above 32% External Quantum Efficiency in Blue Devices, *Adv. Opt. Mater.*, 2018, **6**, 1800385.

126 J. Jin, Y. Tao, H. Jiang, R. Chen, G. Xie, Q. Xue, C. Tao, L. Jin, C. Zheng and W. Huang, Star-shaped boron-containing asymmetric host materials for solution-processable phosphorescent organic light-emitting diodes, *Adv. Sci.*, 2018, **5**, 1800292.

127 C. W. Lu, C. C. Tsai, Y. S. Huang, H. Y. Chih, W. C. Li, T. Y. Chiu and C. H. Chang, Triarylboryl-substituted carbazoles as bipolar host materials for efficient green phosphorescent organic light-emitting devices, *Dyes Pigm.*, 2019, **163**, 145.

128 A. Kumar, J. Oh, J. Kim, J. Jung and M. H. Lee, Facile color tuning of thermally activated delayed fluorescence by substituted *ortho*-carbazole-appended triarylboron emitters, *Dyes Pigm.*, 2019, **168**, 273.

129 A. Kumar, W. Lee, T. Lee, J. Jung, S. Yoo and M. H. Lee, Triarylboron-based TADF emitters with perfluoro substituents: high-efficiency OLEDs with a power efficiency over 100 l m W^{-1}, *J. Mater. Chem. C*, 2020, **8**, 4253.

130 P. Ganesan, D. G. Chen, W. C. Chen, P. Gnanasekaran, J. A. Lin, C. Y. Huang, M. C. Chen, C. S. Lee, P. T. Chou and Y. Chi, Methoxy substituents activated carbazole-based boron dimesityl TADF emitters, *J. Mater. Chem. C*, 2020, **8**, 4780.

131 A. K. Narsaria, F. Rauch, J. Krebs, P. Endres, A. Friedrich, I. Krummenacher, H. Braunschweig, M. Finze, J. Nitsch, F. M. Bickelhaupt and T. B. Marder, Computationally Guided Molecular Design to Minimize the LE/CT Gap in D–π–A Fluorinated Triarylboranes for Efficient TADF via D and π-Bridge Tuning, *Adv. Funct. Mater.*, 2020, **30**, 2002064.

132 X. Dong, H. Wang, J. Huo, S. Liu, H. Shi, F. Cheng and B. Z. Tang, Synthesis, crystal structure, aggregation-induced emission enhancement and electroluminescence properties of a novel compound containing carbazole and triarylborane groups, *J. Mol. Struct.*, 2021, **1228**, 129721.

133 D. Yang, J. M. Kim, J. S. Huh, J. J. Kim and J. I. Hong, The effect of the electron-donor ability on the OLED efficiency of twisted donor-acceptor type emitters, *Org. Electron.*, 2021, **95**, 106187.

134 M. Chen, J. Wei, Y. Zhang, L. Wu, L. Tan, S. Shi, J. Shi and L. Ji, 2,7-Carbazole derived organoboron compounds: synthesis and molecular fluorescence, *Front. Chem.*, 2021, **9**, 754298.

135 X. W. Sun, L. Y. Peng, Y. J. Gao, J. T. Ye and G. Cui, Theoretical studies on boron dimesityl-based thermally activated delayed fluorescence organic emitters: excited-state properties and mechanisms, *New J. Chem.*, 2022, **46**, 15678.

136 H. Ding, Y. Sun, M. Tang, J. Wen, S. Yue, Y. Peng, F. Li, L. Zheng, S. Wang, Y. Shi and Q. Cao, Time-dependent photo-activated aminoborane room-temperature phosphorescence materials with unprecedented properties: simple, versatile, multicolor-tuneable, water resistance, optical information writing/erasing, and multilevel data encryption, *Chem. Sci.*, 2023, **14**, 4633.